DOT/FAA/AR-02/101

Office of Aviation Research
Washington, D.C. 20591

Damage Tolerance Characterization of Sandwich Composites Using Response Surfaces

November 2002

Final Report

U.S. Department of Transportation
Federal Aviation Administration

NOTICE

Technical Report Documentation Page

1. Report No.	2. Government Accession No.	3. Recipient's Catalog No.
DOT/FAA/AR-02/101		

4. Title and Subtitle	5. Report Date
DAMAGE TOLERANCE CHARACTERIZATION OF SANDWICH COMPOSITES USING RESPONSE SURFACES	November 2002
	6. Performing Organization Code

7. Author(s)	8. Performing Organization Report No.
Lacy, T.E., Samarah, I.K., and Tomblin, J.S.	

9. Performing Organization Name and Address	10. Work Unit No. (TRAIS)
Wichita State University 1845 Fairmount Wichita, KS 67260-0044	
	11. Contract or Grant No. GA05

12. Sponsoring Agency Name and Address	13. Type of Report and Period Covered
U.S. Department of Transportation Federal Aviation Administration Office of Aviation Research Washington, DC 20591	Final Report
	14. Sponsoring Agency Code ACE-110

15. Supplementary Notes

The FAA William J. Hughes Technical Center COTR was Peter Shyprykevich.

16. Abstract

The influence of material configuration and impact parameters on the damage tolerance characteristics of sandwich composites comprised of carbon-epoxy woven fabric facesheets and Nomex honeycomb cores was investigated using empirically based response surfaces. A series of carefully selected tests were used to isolate the coupled influence of various combinations of the number of facesheet plies, core density, core thickness, impact energy, impactor diameter, and impact velocity on the residual strength degradation due to vertical impact. The ranges of selected material parameters were typical of those found in common aircraft applications. Quadratic response surface estimates of the compressive residual strength as a continuous function of sandwich configuration and impact parameters did not correlate as well as impact resistance because of bifurcations between failure modes. For a fixed set of impact parameters, regression results suggest that impact damage development and residual strength degradation is highly sandwich configuration dependent. Increasing the number of facesheet plies and the thickness of the core material resulted in the greatest improvement in the damage tolerance characteristics. An increase in the impactor diameter and impact energy results in a significant decrease in the estimated residual strength, particularly for those sandwich panels with thicker facesheets. The effects of impact velocity on damage formation and loss of strength were also addressed. The developed response surfaces for the compressive residual strength may have limited use, particularly as the measured data at low- energy impact levels, small impactor diameter, and thin facesheets exhibit significant scatter. Employing the methodology outlined here, it may be possible to tailor sandwich composite designs in order to obtain enhanced damage tolerance characteristics over a range of expected impacts. Such efforts may facilitate sandwich panel design by establishing relationships between sandwich configuration and impact parameters that lead to improved damage tolerance/resistance.

17. Key Words	18. Distribution Statement
Composites, Sandwich, Honeycomb, Damage tolerance, Impact, Response surface, Residual strength	This document is available to the public through the National Technical Information Service (NTIS), Springfield, Virginia 22161.

19. Security Classif. (of this report)	20. Security Classif. (of this page)	21. No. of Pages	22. Price
Unclassified	Unclassified	47	

TABLE OF CONTENTS

LIST OF FIGURES

LIST OF TABLES

EXECUTIVE SUMMARY

The influence of material configuration and impact parameters on the damage tolerance characteristics of sandwich composites comprised of carbon-epoxy woven fabric facesheets and Nomex honeycomb cores was investigated using empirically based response surfaces. A series of carefully selected tests were used to isolate the coupled influence of various combinations of the number of facesheet plies, core density, core thickness, impact energy, impactor diameter, and impact velocity on the residual strength degradation due to normal impact. The ranges of selected material parameters were typical of those found in common aircraft applications. Quadratic response surface estimates of the compressive residual strength as a continuous function of material system and impact parameters did not correlate as well as impact resistance because of bifurcations between failure modes. For a fixed set of impact parameters, regression results suggest that impact damage development and residual strength degradation is highly sandwich configuration dependent. Increasing the number of facesheet plies and the thickness of the core material resulted in the greatest improvement in the damage tolerance characteristics. An increase in the impactor diameter and impact energy results in a significant decrease in the estimated residual strength, particularly for those sandwich panels with thicker facesheets. The effects of impact velocity on damage formation and loss of strength were also addressed. The development response surfaces for the compressive residual strength may have limited use, particularly as the measured data at low-energy impact levels, small impactor diameter, and thin facesheets exhibit significant scatter. Employing the methodology outlined here, it may be possible to tailor sandwich composite designs to obtain enhanced damage tolerance characteristics over a range of expected impacts. Such efforts may facilitate sandwich panel design by establishing relationships between sandwich configuration and impact parameters that lead to improved damage tolerance and resistance.

1. INTRODUCTION.

Sandwich construction composites are used in a wide variety of structural applications largely because of their relative advantages over other structural materials in terms of improved stability and weight savings. Sandwich plates and shells are multilayered structures consisting of one or more high-strength, stiff layers (e.g., laminated facings) that are bonded to one or more flexible layers (core), as shown in figure 1. While the initial design of composite sandwich structures is at a fairly mature stage of development [1-3], less progress has been made in understanding the effect of adverse in-service impact events on the structural integrity of such structures. Such an understanding is critical if there is to be widespread use of sandwich composites in applications where structural durability and damage tolerance are primary considerations (e.g., aerospace or automotive applications). Low-energy impacts may induce localized damage in sandwich composites (fiber breaks, resin cracking, face sheet-core delamination, core crush, puncture, etc.) and can be attributable to a number of fairly common discrete sources (hail, tool drops, runway projectiles, bird strikes, or other unintentional impacts). Any reference to impact damage used herein will suggest the damage associated with relatively low-energy and low-velocity impact events. The effect of intrinsic processing induced defects (porosity, voids, small disbonds, etc.) and catastrophic damage associated with high-energy impacts resulting from airplane crashes or similar events are not considered here.

Characterizing the thermomechanical response of sandwich composites with varying levels of impact damage is a crucial issue in the development of a damage tolerance plan for composite structures. Foreign object impact damage in sandwich composites may result in drastic reductions in strength, elastic moduli, and durability and damage tolerance characteristics. An overview of recent investigations into the mechanics of damaged composites may be found in references 4-13. The motivation for this study is the development of empirically based models (i.e., "response surfaces") that isolate the influence of key sandwich configuration parameters (e.g., number of facesheet plies or facesheet thickness, core thickness, and core density) and impact parameters (e.g., impact energy, spherical impactor diameter, and impact velocity) on the damage tolerance characteristics of sandwich composites. This effort extends the work of Lacy et al. [13], which developed response surfaces for assessing the impact damage resistance properties of sandwich composites. This study represents a subset of a somewhat larger investigation into the durability and damage tolerance properties of sandwich composites with varying levels of impact damage [4, 5, 12, and 13]. The focus of this examination is on sandwich composites comprised of plain weave carbon-epoxy facesheets and Nomex honeycomb cores subjected to compression after impact (CAI) loading.

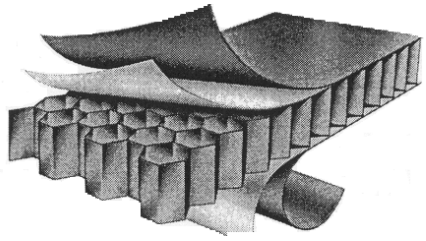

FIGURE 1. TYPICAL SANDWICH COMPOSITE CONSTRUCTION FORM

2. DAMAGE TOLERANCE CHARACTERIZATION USING EXPERIMENTALLY DETERMINED RESPONSE SURFACES.

In this study, symmetric flat composite sandwich panels comprised of plain-weave carbon fabric preimpregnated in epoxy resin (NEWPORT NB321/3K70P) facesheets and Plascore Nomex honeycomb (PN2-3/16-3.0/4.5/6.0) cores (test section dimensions, 8.0 in x 8.0 in) with clamped edges were subjected to drop-weight vertical impact with a spherical steel impactor followed by CAI testing [5]. Three different facesheet configurations, (X_1 = 2 plies $[90/45]_1$, 4 plies $[90/45]_2$, 6 plies $[90/45]_3$), core densities (X_2 = 3.0, 4.5, 6.0 lb/ft^3), and core thicknesses (X_3 = 3/8, 3/4, and 9/8 in) were considered in this examination. The ranges of material system variables are typical of those found in common sandwich panel applications. In addition, three different impact energies (X_4 = 90.0, 120.0, 150.0 in-lbs), impactor diameters (X_5 = 1.0, 2.0, 3.0 in), and impact velocities (X_6 = 65.21, 96.3, 127.39 in/s) were considered in this study. The impact parameters correspond to typical low-velocity impacts associated with relatively blunt objects. Note that each sandwich configuration and impact variable, X_i (i = 1, 2,.., 6), assumes low, midrange or center point, and high values which are collectively referred to as the natural values of the independent variables used in this study. Table 1 summarizes the range of material and impact parameters considered in this effort. In addition, the facesheet thickness may be characterized in terms of the number of plies (2, 4, 6) associated with each facesheet configuration.

TABLE 1. SANDWICH CONFIGURATION AND IMPACT PARAMETERS

		Natural Values		
Material Variables	Number of Facesheet Plies, X_1	2 $[90/45]_1$	4 $[90/45]_2$	6 $[90/45]_3$
	Core Density, X_2 (lb/ft^3)	3.0	4.5	6.0
	Core Thickness, X_3 (in)	0.375	0.750	1.125
Impact Variables	Impact Energy, X_4 (in-lbs)	90.0	120.0	150.0
	Impactor Diameter, X_5 (in)	1.0	2.0	3.0
	Impact Velocity, X_6 (in/s)	65.21	96.30	127.39

Earlier efforts [5 and 13] used through transmission ultrasonic (TTU) C-scan measurements and maximum residual facesheet indentation measurements to characterize the degree of impact damage induced in the sandwich panels. TTU C-scan measurements provide a two-dimensional (2D) image of the projected area of the impact-damaged region, as shown in figure 2. The damage region may be characterized either in terms of the area of the C-scan image or in terms of the diameter of the damaged region, D, measured normal to the direction of the applied CAI load. The latter represents an estimate of the region around which stress redistribution due to the presence of damage must occur.

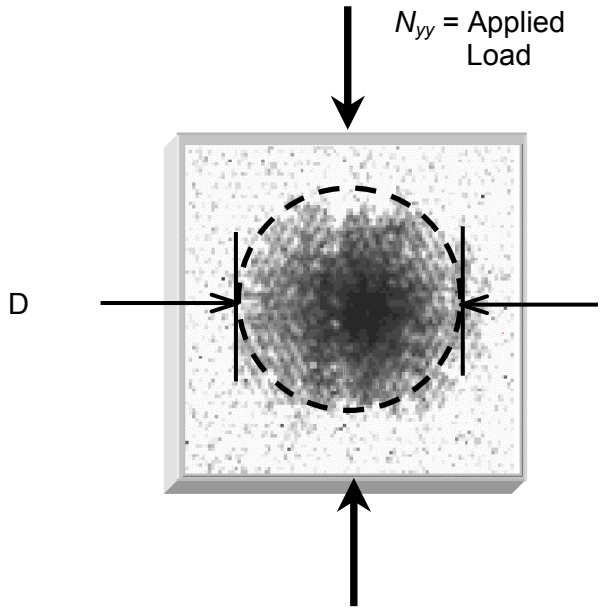

FIGURE 2. TTU C-SCAN IMAGE

Destructive sectioning of impact-damaged sandwich composites comprised of low-density Nomex honeycomb cores (X_2 = 3.0 lb/ft^3) of variable thickness (X_3 = 3/8, 3/4 in) shows that, for the given facesheet configurations, the planar damage region based upon TTU C-scan measurements closely corresponds to the region over which Nomex honeycomb cell wall buckling/fracture occurs [5]. Furthermore, Tomblin et al. [5] demonstrated the CAI residual strength of such sandwich composites correlated reasonably well with the projected damage area based upon TTU C-scan measurements for normal impacts involving a range of impactor diameters and impact energies. For example, figure 3 shows the normalized CAI residual strength as a function of projected damage area for symmetric sandwich composites comprised of woven fabric carbon-epoxy facesheets (X_1 = 2 plies $[90/45]_1$, 4 plies $[90/45]_2$, 6 plies $[90/45]_3$) and low-density Nomex honeycomb cores (X_2 = 3.0 lb/ft^3) of variable thickness (X_3 = 3/8, 3/4 in) from [5]. The panels were impacted with either 1.0 or 3.0 in outside diameter (OD) impactors over a range of impact energies. The CAI residual strength of each damaged panel was normalized by the CAI residual strength of an undamaged (virgin) panel of identical facesheet configuration. It is clear from the figure that the normalized CAI residual strength is a generally decreasing function of the projected damage area, but with substantial scatter. In addition, the greatest degradation in CAI residual strength is typically associated with those panels impacted with a 3.0 in OD impactor. This latter result is of particular concern because sandwich panels impacted with relatively blunt impactors often display relatively low levels of visible facesheet damage [5 and 13]. For the sandwich panels considered in this study, Lacy et al. [13] previously developed response surfaces for estimating the planar dimension of the region with crushed core as well as the residual facesheet indentation. For a detailed description of the experimental setup and procedure, impact testing, nondestructive and destructive damage evaluation, and CAI testing associated with this effort, please see reference 5.

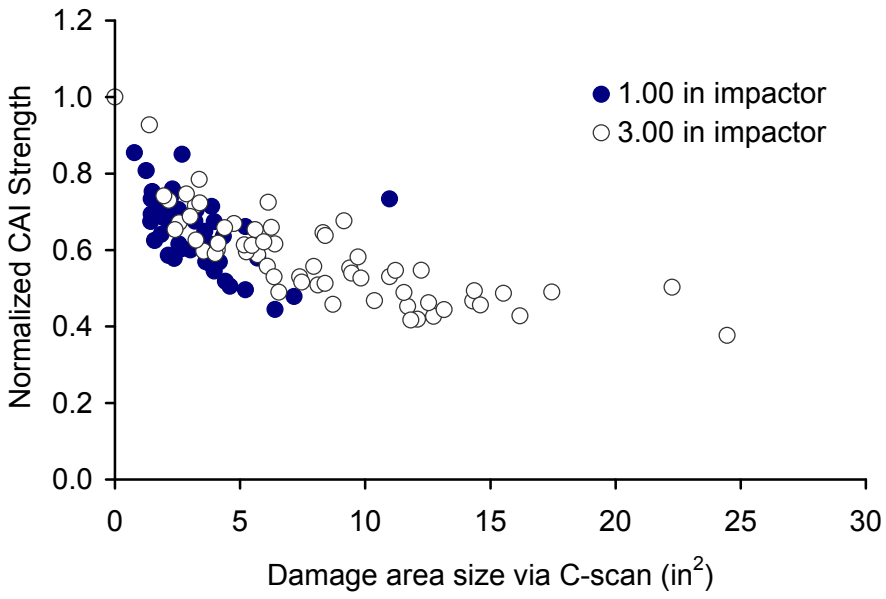

FIGURE 3. NORMALIZED CAI RESIDUAL STRENGTH AS A FUNCTION OF TTU C-SCAN AREA FROM REFERENCE 5

One primary goal of this study is to develop empirically based models (i.e., response surfaces) that isolate the influence of key sandwich configuration parameters (e.g., number of facesheet plies or facesheet thickness, X_1; core density, X_2; and core thickness, X_3) and impact parameters (e.g., impact energy, X_4; spherical impactor diameter, X_5; and impact velocity, X_6) on the damage tolerance properties of sandwich composites. The diameter, D, of the TTU C-scan area will primarily be used to characterize the level of impact damage (cf., figure 2). Lacy et al. [13] demonstrated that there may be no correlation between the residual indentation depth (e.g., visible damage) and the size of the internal core crush region. Combinations of independent variables, X_1 through X_6, leading to a reduced value of the diameter, D, of the projected C-scan area for a given impact event may minimize the degradation in the normalized CAI residual strength for a given panel configuration.

The damage-induced residual strength degradation in sandwich composites due to foreign object impact is highly configuration and impact parameter dependent. Three distinct sets of 15 experiments were conducted to isolate the effects of (1) sandwich configuration/layup parameters (X_1 through X_3); (2) the number of facesheet plies (X_1), impact energy (X_4), and impactor diameter (X_5); and (3) the number of facesheet plies (X_1), impact energy (X_4), and impact velocity (X_6) on the damage tolerance characteristics of sandwich composite panels. In each set of experiments, three of the independent variables were tested at the low, center point, and high natural levels defined in table 1, while the remaining independent variables were held fixed.

2.1 INFLUENCE OF SANDWICH CONFIGURATION PARAMETERS ON THE IMPACT DAMAGE TOLERANCE OF SANDWICH COMPOSITES.

Similar to reference 13, a 3^k fractional factorial design of experiments (DOE) approach [14] was used to examine the nonlinear interaction effects between relevant sandwich panel design parameters and their influence on the CAI residual strength, N_{yy}, associated with a given impact event. To isolate the coupled effects of sandwich configuration parameters (i.e., number of facesheet plies, X_1; core density, X_2; core thickness, X_3) on the damage tolerance characteristics of sandwich composite panels, the impact energy ($X_4 = 120.0$ in-lbs), impactor diameter ($X_5 = 3.0$ in), and impact velocity ($X_6 = 96.30$ in/s) were held fixed in this examination. Based on a number of carefully selected experiments, statistically reliable polynomial expressions characterizing the impact damage response of sandwich composites may be determined as a continuous function of relevant test parameters [cf., 14-19]. A quadratic response surface generally will be of the form

$$\hat{Y} = b_0 + \sum_{i=1}^{k} b_i \cdot x_i + \sum_{i=1}^{k} \sum_{j=1}^{k} b_{ij} \cdot x_i \cdot x_j \tag{1}$$

where $\hat{Y}$ is the predicted response quantity of interest (e.g., residual strength); x_i are continuous normalized independent variables; b_0, b_i, and b_{ij} are least squares regression coefficients; and k denotes the number of independent variables considered in the test. The three natural values of the independent variables, X_i, (corresponding to low, center point, and high values) are mapped into three nondimensionalized or coded levels, x_i, corresponding to (-1, 0, 1), respectively. In general, the relationship between the natural value and coded level of a given independent variable may be expressed as

$$x_i = \frac{2 \cdot X_i - (X_{iMAX} + X_{iMIN})}{(X_{iMAX} - X_{iMIN})} \tag{2}$$

where X_{iMIN} and X_{iMAX} correspond to the low and high natural values of the i^{th} independent variable, respectively. Equation 1 represents a quadratic surface in the k-dimensional space of input parameters; (x_1, x_2, ... x_i, ..., x_k) = (0, 0, …, 0, …, 0) defines the center point of the test matrix design where the independent variables are tested at their midrange values. The constant b_0 represents the average response at the center point of the design, while b_i and b_{ij} contribute to the deviation from this average value at points removed from the center point ($i, j = 1, 2, \ldots, k$). The test matrices are selected so the generated response surfaces exhibit a high degree of orthogonality (i.e., only b_0 and b_{ii} are correlated) and rotatability (i.e., the variance of the predicted values at all points equidistant from the center point is constant). One key advantage of this approach is that it can estimate the impact damage responses associated with specific sandwich panel configurations, which was not originally tested. In addition, the coupling and interactions between input parameters and their influence on the desired response, $\hat{Y}$, may be directly inferred from the magnitudes of the coefficients, b_{ij} ($i \neq j$).

The test matrix developed for this investigation is based on the Box-Behnken fractional factorial design of experiments technique which uses the minimum number of tests required to generate a

second-order, statistically reliable, polynomial expression characterizing the response function of interest (e.g., residual strength) [14]. Similar approaches have been used to characterize the fracture toughness, residual strength, and damage tolerance characteristics of composite laminates [20-22]. Table 2 summarizes the natural values and coded levels of the ($k = 3$) independent variables considered in this study. Defining the CAI residual strength as the desired response quantity, $\hat{N}_{yy}$, equation 1 may be expressed in expanded form, i.e.,

$$\hat{N}_{yy} = b_0 + b_1 \cdot x_1 + b_2 \cdot x_2 + b_3 \cdot x_3 + b_{11} \cdot x_1^2 + b_{22} \cdot x_2^2 + b_{33} \cdot x_3^2 \\ \ldots + b_{12} \cdot x_1 \cdot x_2 + b_{13} \cdot x_1 \cdot x_3 + b_{23} \cdot x_2 \cdot x_3 \tag{3}$$

where x_i is the coded level of the i^{th} independent variable (i = 1, 2, 3). Note that the estimate of residual strength in equation 3 is a continuous function of independent variables. Such a representation may be inappropriate where the range of independent variables spans a bifurcation between failure modes (e.g., a transition from facesheet fracture to facesheet dimple propagation). This may be a serious concern where changes in facesheet penetration resistance associated with variations in the number of facesheet plies, impactor diameter, or impact energy may lead to multiple CAI failure mechanisms.

TABLE 2. NATURAL VALUES AND CORRESPONDING CODED LEVELS OF MATERIAL SYSTEM VARIABLES

i	Material Variable	Natural Value, X_i	Coded Level, x_i
1	Number of Facesheet Plies	2 $[90/45]_1$	-1
		4 $[90/45]_2$	0
		6 $[90/45]_3$	+1
2	Core Density	3.0 lb/ft^3	-1
		4.5 lb/ft^3	0
		6.0 lb/ft^3	+1
3	Core Thickness	0.375 in	-1
		0.750 in	0
		1.125 in	+1

Consistent with reference 13, the experimental matrix used in this study to solve for the regression coefficients (b_0, b_i, and b_{ij}; i, j = 1, 2, 3) required that the high- and low-coded levels of any two independent variables be paired in all possible combinations while fixing the third independent variable at its coded center point level. These tests are performed in combination with three additional experiments in which the independent variables are fixed at their center point values ($x_1 = x_2 = x_3 = 0$), resulting in a total of 15 experiments. The latter three center runs are important for assessing the degree of curvature in the response as well as for evaluating model error and goodness of fit. Table 3 shows the test matrix used in this evaluation in terms of the coded levels of the independent variables as well as the measured residual strength, N_{yy}, associated with each test. The regression coefficients should be selected so the error between the

predicted values of residual strength, $\hat{N}_{yy}$, and the experimentally observed values, N_{yy}, is minimized over the range of panel configurations tested.

Using the methodology outlined by Lacy et al. [13], the vector of desired regression coefficients,

$$\{b\}=\left(b_0,b_1,b_2,b_3,b_{11},b_{22},b_{33},b_{12},b_{13},b_{23}\right)^T \tag{4}$$

may be determined from

$$b=\left(x^T\cdot x\right)^{-1}\cdot\left(x^T\cdot N_{yy}\right) \tag{5}$$

where $\{N_{yy}\}=\left(N_{yy1},N_{yy2},...,N_{yy15}\right)^T$ is a vector containing the experimentally observed responses (i.e., the measured residual strengths from the fifth column in table 3), and the matrix, x, has components

$$[[x]]=\begin{bmatrix} 1 & x_1^{(1)} & x_2^{(1)} & x_3^{(1)} & \left(x_1^{(1)}\right)^2 & \left(x_2^{(1)}\right)^2 & \left(x_3^{(1)}\right)^2 & x_1^{(1)}\cdot x_2^{(1)} & x_1^{(1)}\cdot x_3^{(1)} & x_2^{(1)}\cdot x_3^{(1)} \\ 1 & x_1^{(2)} & x_2^{(2)} & x_3^{(2)} & \left(x_1^{(2)}\right)^2 & \left(x_2^{(2)}\right)^2 & \left(x_3^{(2)}\right)^2 & x_1^{(2)}\cdot x_2^{(2)} & x_1^{(2)}\cdot x_3^{(2)} & x_2^{(2)}\cdot x_3^{(2)} \\ \vdots & \vdots & \vdots & \vdots & \vdots & \vdots & \vdots & \vdots & \vdots & \vdots \\ 1 & x_1^{(15)} & x_2^{(15)} & x_3^{(15)} & \left(x_1^{(15)}\right)^2 & \left(x_2^{(15)}\right)^2 & \left(x_3^{(15)}\right)^2 & x_1^{(15)}\cdot x_2^{(15)} & x_1^{(15)}\cdot x_3^{(15)} & x_2^{(15)}\cdot x_3^{(15)} \end{bmatrix} \tag{6}$$

where $x_i^{(k)}$ represents the specified coded level of the i^{th} independent variable (i = 1, 2, 3) during the k^{th} experimental run (k = 1, 2, …, 15) from table 3.

The vector, b, is commonly referred to as the least squares estimate of the model parameters vector. This estimate is unbiased and has the minimum variance among all other types of unbiased estimators [17]. Using equations 5 and 6 in combination with the vector, N_{yy}, of observed responses from table 3, the quadratic response surface in equation 3 characterizing the CAI residual strength as a continuous function of coded levels of the composite sandwich panel facesheet thickness (x_1), core density (x_2), and core thickness (x_3) may be expressed as

$$\begin{aligned} \hat{N}_{yy} &= 2149+937.0\cdot x_1+103.0\cdot x_2+424.9\cdot x_3 \\ &\quad ...+5.770\cdot x_1^2-190.3\cdot x_2^2-265.3\cdot x_3^2 \qquad \text{(lbs/in)} \\ &\quad ...-55.09\cdot x_1\cdot x_2+442.1\cdot x_1\cdot x_3+6.380\cdot x_2\cdot x_3 \end{aligned} \tag{7}$$

The constant term (b_0 = 2149 lbs/in) represents the mean CAI residual strength for those panels corresponding to the center point of the design. Note that based upon the magnitudes of the coefficients of the linear terms in equation 7, the coded number of facesheet plies, x_1, contributes the most to the linear variation in the predicted response at points removed from the center point (x_1, x_2, x_3) = (0, 0, 0) of the designed test matrix (e.g., increasing the number of plies from its midrange value will result in a linear increase in the predicted residual strength from b_0;

conversely, decreasing the number of plies from its midrange value will result in a linear decrease in the predicted response). It makes sense that, for a given impact event, panels with a greater number of facesheet plies will have a relatively higher CAI residual strength. Similarly, an increase in the core density, x_2, or in the core thickness, x_3, will contribute to a linear increase in the residual strength. Based upon the coefficients of the quadratic terms, variations in the coded core density or core thickness away from their midrange values will result in a modest quadratic decrease in the predicted CAI residual strength.

Due to the normalization procedure used in defining the coded variables (equation 2), the influence of the quadratic terms on the predicted response will be maximized as the coded variables approach their extreme values ($x_i = \pm 1$). The coefficients of the interaction terms ($x_i \cdot x_j;\ i \neq j$) provide an indication of the complex coupling between material parameters and their influence on the sandwich panel damage tolerance characteristics. In this case, a simultaneous increase in the number of facesheet plies and core thickness will have a beneficial effect on the predicted response. Similar arguments can be made when interpreting the influence the remaining terms in equation 7 has on the predicted response. It is clear from the functional form of the response surface, (equation 7), that for the given range of material and impact parameters, the CAI residual strength is somewhat sandwich configuration dependent.

Note that the Box-Behnken test matrix defined in table 3 represents a spherical experimental design, i.e., the first 12 tests are conducted at points (x_1, x_2, x_3) that are equidistant from the center point of the design. If one considers a cube in the space of the coded variables defined by the planes ($x_1 = \pm 1$, $x_2 = \pm 1$, $x_3 = \pm 1$), the noncenter point tests are conducted at edge points (i.e., points located at the centers of the edges of the cube) as shown schematically in figure 4. Hence, the edge points all lie a coded radial distance, $r = \sqrt{x_1^2 + x_2^2 + x_3^2} = \sqrt{2} = 1.414$, from the center point of the design. When using response surfaces, such as equation 7, to estimate the impact damage response associated with panel configurations not considered in the original test matrix, special care must be used to ensure that the interpolation occurs within the spherical domain defined by the coded radius, $r = \sqrt{2}$. Extrapolation to panel configurations that lie outside of this spherical region may lead to serious errors in the predicted response. If response surface estimates are desired over a cuboidal domain, then various other experimental designs may be used (e.g., Central Composites Design; cf. [17]).

While the interpretation of the regression coefficients is most easily performed if a response surface is characterized in terms of the coded levels of the independent variables, equation 2 may be used to rewrite the response surface in equation 7 in terms of the natural values of the independent variables, i.e.,

$$\begin{aligned} \hat{N}_{yy} = & -2159 + 97.56 \cdot X_1 + 894.7 \cdot X_2 + 1554 \cdot X_3 \\ & \ldots + 1.441 \cdot X_1^2 - 84.56 \cdot X_2^2 - 1887 \cdot X_3^2 \qquad \text{(lbs/in)} \qquad (8) \\ & \ldots - 18.36 \cdot X_1 \cdot X_2 + 589.4 \cdot X_1 \cdot X_3 + 11.35 \cdot X_2 \cdot X_3 \end{aligned}$$

The latter representation allows the response surface to be plotted in the space of the natural variables. The response surface (equation 7 or 8) may be used to identify those panel configurations that retain a higher fraction of their virgin panel strength for a given impact event.

Table 3 summarizes the measured and predicted CAI residual strength for the sandwich composite panels considered in this study. The difference between the experimentally measured CAI strengths and the estimated values using equation 7 varied between 0.4% and 9.1% for the 15 panels tested, with a mean difference of 3.4%. This suggests that the response surface (equation 7) may provide a reasonable characterization of the influence of the number facesheet plies, core density, and core thickness on CAI residual strength. It is useful to recognize that those specimens with two-ply facesheet configurations (x_1 = -1) showed the biggest disparity between the measured and estimated CAI residual strengths. The regression results may also be viewed schematically in the space of coded independent variables, as shown in figure 4. Note that the experimental center point observations (cf., table 3) are tightly banded about their mean value, b_0 = 2149 lbs/in. This is highly desirable in order to avoid introducing a large degree of uncertainty into the regression model. This can be a particular concern where the experimental observations may not be particularly repeatable. Standard analysis of variance, error estimation, and goodness of fit checks [17] suggest that the response surface in equation 7 provides a statistically reliable estimate of CAI residual strength.

TABLE 3. CODED SANDWICH CONFIGURATION VARIABLES TEST MATRIX AND MEASURED AND PREDICTED RESIDUAL STRENGTH

Test, k	x_1	x_2	x_3	Measured Residual Strength, N_{yy} (lbs/in)	Predicted Residual Strength, $\hat{N}_{yy}$ (lbs/in)	$\left\lvert \frac{N_{yy} - \hat{N}_{yy}}{N_{yy}} \right\rvert$ (%)
1	+1	+1	0	2996	2949	1.6
2	+1	-1	0	2952	2853	3.3
3	-1	+1	0	1087	1185	9.1
4	-1	-1	0	822.2	868.9	5.7
5	+1	0	+1	3637	3693	1.5
6	+1	0	-1	1870	1959	4.8
7	-1	0	+1	1024	934.7	8.7
8	-1	0	-1	1025	969.2	5.5
9	0	+1	+1	2236	2227	0.4
10	0	+1	-1	1407	1365	3.0
11	0	-1	+1	1966	2008	2.2
12	0	-1	-1	1162	1172	0.8
13	0	0	0	2107	2149	2.0
14	0	0	0	2182	2149	1.5
15	0	0	0	2157	2149	0.4

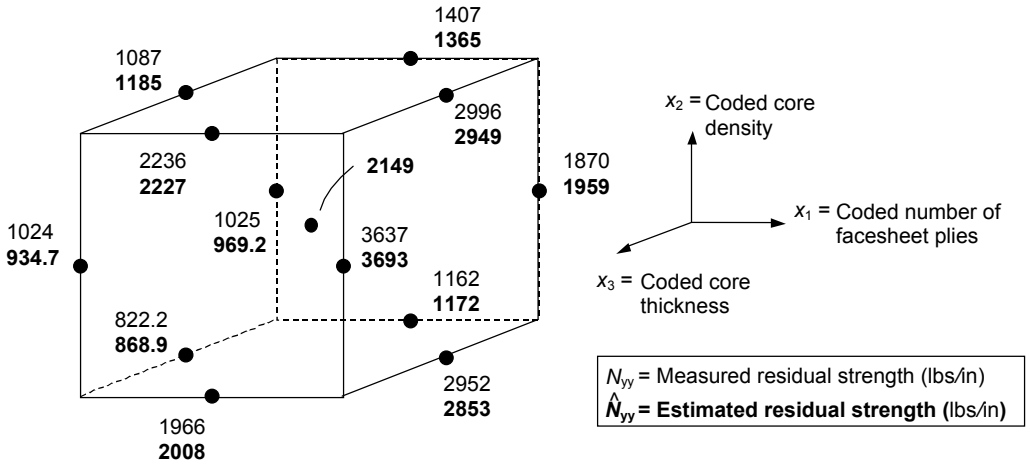

FIGURE 4. RESPONSE SURFACE ESTIMATES OF RESIDUAL STRENGTH AS A FUNCTION OF SANDWICH CONFIGURATION PARAMETERS

Figure 5 summarizes the influence the number of facesheet plies (X_1, x_1), core density (X_2, x_2), and core thickness (X_3, x_3) have on the estimate of CAI residual strength (equation 8) for a fixed impact energy, impactor diameter and velocity. In the response surface plots, the bounds of the sphere of coded radius, $r = \sqrt{2}$, is denoted by an inscribed dashed circle. Strictly speaking, regression data falling outside the bounds of this sphere would correspond to an extrapolation of the response surface results. Figures 5(a), 5(b), and 5(c) show the CAI residual strength (equation 8) as a function of core density and core thickness for the two-ply, four-ply, and six-ply facesheet configurations (or x_1 = -1, 0, 1), respectively. A comparison of the three figures reveals that the predicted strength increases substantially as the number of facesheet plies is increased. It is clear from figure 5(a), that for sandwich panels with the minimum number of facesheet plies (X_1 = 2 plies; x_1 = -1), the CAI strength generally increases with increasing core density, X_2. The CAI strength is a relative maximum in the vicinity of the maximum core density (X_2 = 6.0 lb/ft^3; x_2 = 1) and midrange core thickness (X_3 = 3/4 in; x_3 = 0). The minimum strength occurs in the vicinity of X_2 = 3.0 lb/ft^3 (x_2 = -1) and X_3 = 3/4 in (x_3 = 0). The relatively reduced penetration resistance associated with the two-ply facesheet configuration likely results in more localized damage development for a given impact event, particularly as the core density is decreased.

As the number of facesheet plies is increased to its midrange value (X_1 = 4 plies; x_1 = 0), the magnitude of the peak CAI strength and its location in the space of independent variables changes (figure 5(b)). The estimated CAI strength tends to increase rapidly with increasing core thickness and is less sensitive to the density of the core. For the relatively blunt object impacts considered here, enhanced penetration resistance associated with an increase in the number of facesheet plies often results in CAI failure processes characterized by facesheet dimple propagation across the width of the test specimen [5]. The applied load level (e.g., strength), at which this process initiates, apparently is influenced by core thickness (e.g., increasing the core thickness may provide enhanced bending rigidity that serves to delay the onset of facesheet dimple propagation). Here the peak predicted CAI strength occurs in the vicinity of X_2 = 6.0 lb/ft^3 (x_2 = 1) and X_3 = 9/8 in (x_3 = 1); the strength is a relative minimum for

$X_2 = 3.0$ lb/ft^3 ($x_2 = -1$) and $X_3 = 3/8$ in ($x_3 = -1$), corresponding to the extreme ranges of the tested values.

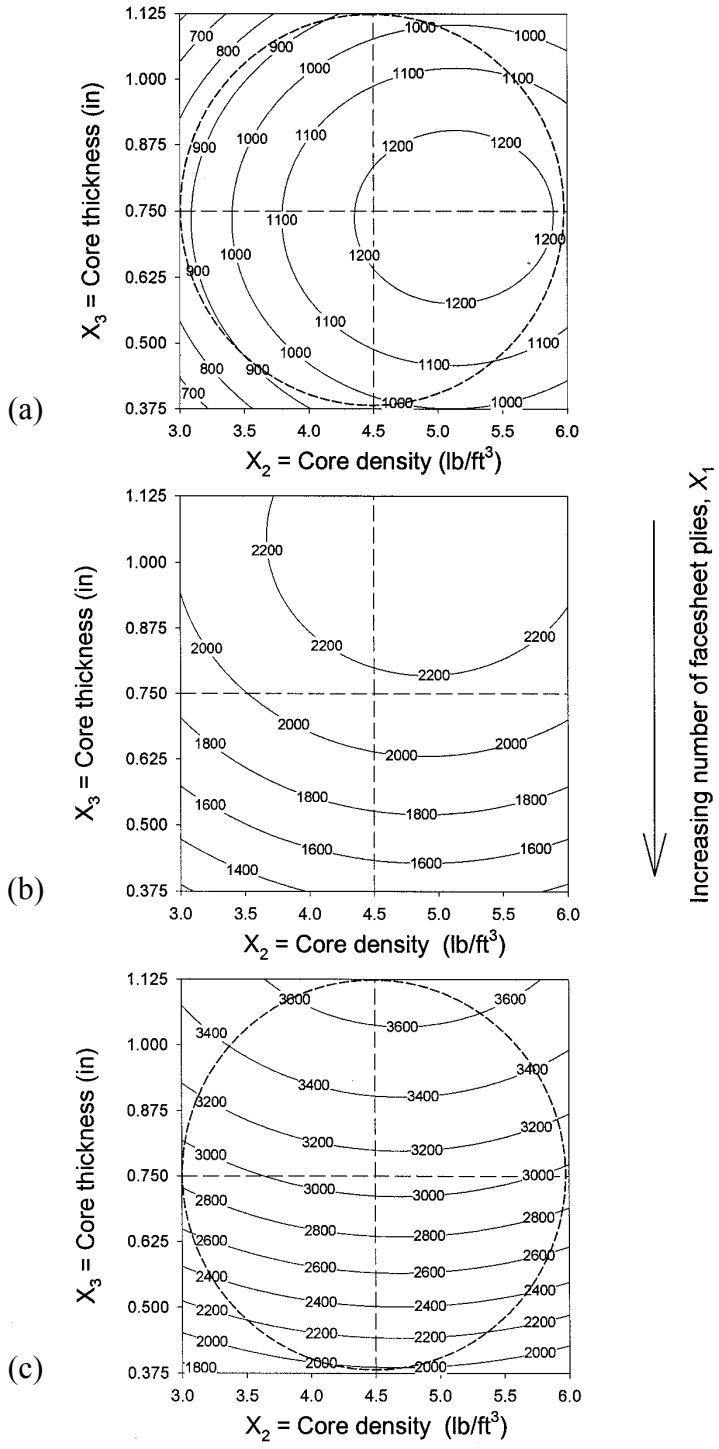

FIGURE 5. PREDICTED RESIDUAL STRENGTH (lbs/in): (a) $X_1 = 2$ plies $[90/45]_1$, (b) $X_1 = 4$ plies $[90/45]_2$, AND (c) $X_1 = 6$ plies $[90/45]_3$

Figure 5(c) shows that for sandwich panels with six-ply facesheet configurations ($X_1 = 6$ plies; $x_1 = 1$), the estimated CAI strength increases significantly with increasing core thickness and is fairly insensitive to core density. There is likely a competition between enhanced penetration resistance and improved bending stiffness associated with changes in independent variables that govern the damage development [13] and residual strength.

The preceding results are in agreement with the experimental observations. Figures 6 through 8 show the recorded CAI residual strengths for the test specimens corresponding to the midrange core thickness configurations ($x_3 = 0$; $X_3 = 3/4$ in), midrange core density configurations ($x_2 = 0$; $X_2 = 4.5$ lb/ft^3), and midrange facesheet configurations ($x_1 = 0$; $X_1 = 4$ plies), respectively. Included with each observation is its associated TTU C-scan image and measured diameter, D, from reference 13. These figures suggest that the experimentally observed CAI strengths for a given facesheet configuration are consistent with the regressions in figure 5. Furthermore, the observed CAI strengths for the four-ply and six-ply facesheet configurations generally were inversely proportional to the diameter of the TTU C-scan images reported in reference 13.

For the test matrix summarized in table 3, figure 9 contains a comparison of the response surface predictions of the TTU C-scan diameter from reference 13 to the response surface predictions of CAI residual strength developed in this examination. For illustration purposes, the CAI residual strength of each damaged panel was normalized by the CAI residual strength of an undamaged (virgin) panel of identical facesheet configuration prior to determination of the regression coefficients (equation 5). A comparison of figures 9(a), 9(b), and 9(c) to figures 9(d), 9(e), and 9(f), respectively, suggests that with the exception of the two-ply facesheet configuration (figures 9(a) and 9(d)), the predicted normalized CAI residual strength is generally inversely proportional to the size of the planar damage area, D, for the given impact. This is consistent with the observations of Tomblin et al. [5] (cf., figure 2). Lacy et al. [13] noted that the reduced penetration resistance associated with the two-ply facesheet configurations likely resulted in a decrease in the planar size of the internal damage for a given impact event. There may be, however, appreciably more localized facesheet damage (ply fracture, fiber breaks, matrix cracks, etc.) that reduces the facesheet load transfer across the impact site. The loss of load carrying capability of the facesheet coupled with the reduced bending stiffness associated with the two-ply facesheet configuration results in a bifurcation between compressive failure modes (i.e., facesheet fracture occurs rather than progressive facesheet dimple propagation). Hence, there may be no clear correlation between the measured TTU C-scan diameter and residual strength for impacts involving partial facesheet penetration. Clearly, using continuous function response surfaces to predict residual strength should be used with extreme caution over ranges of independent variables where a potential bifurcation between failure modes may result in an apparent step discontinuity in the actual residual strength, particularly for those impacts involving smaller diameter impactors, increasing impact energy, and/or thinner facesheets. This may explain why the disparity between the measured and predicted CAI residual strengths was the greatest for sandwich composites with two-ply facesheet configurations (cf., table 3). Similar to the results shown in figure 5, the estimated residual strength for the four-ply and six-ply facesheet configurations may increase significantly with increasing core thickness.

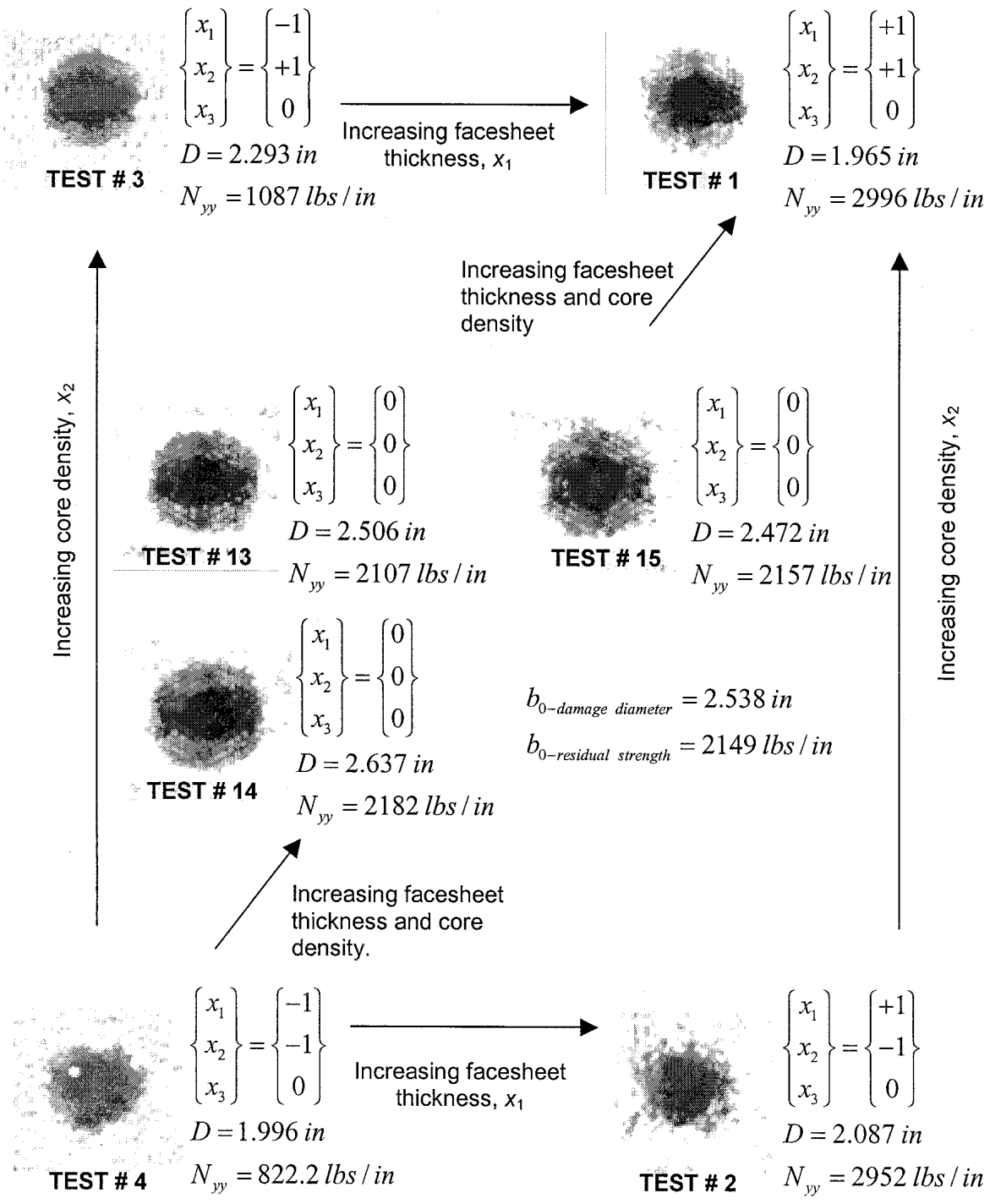

FIGURE 6. MEASURED DAMAGE DIAMETER [13] AND RESIDUAL STRENGTH FOR CORE THICKNESS, X_3 = 3/4 in (x_3 = 0)

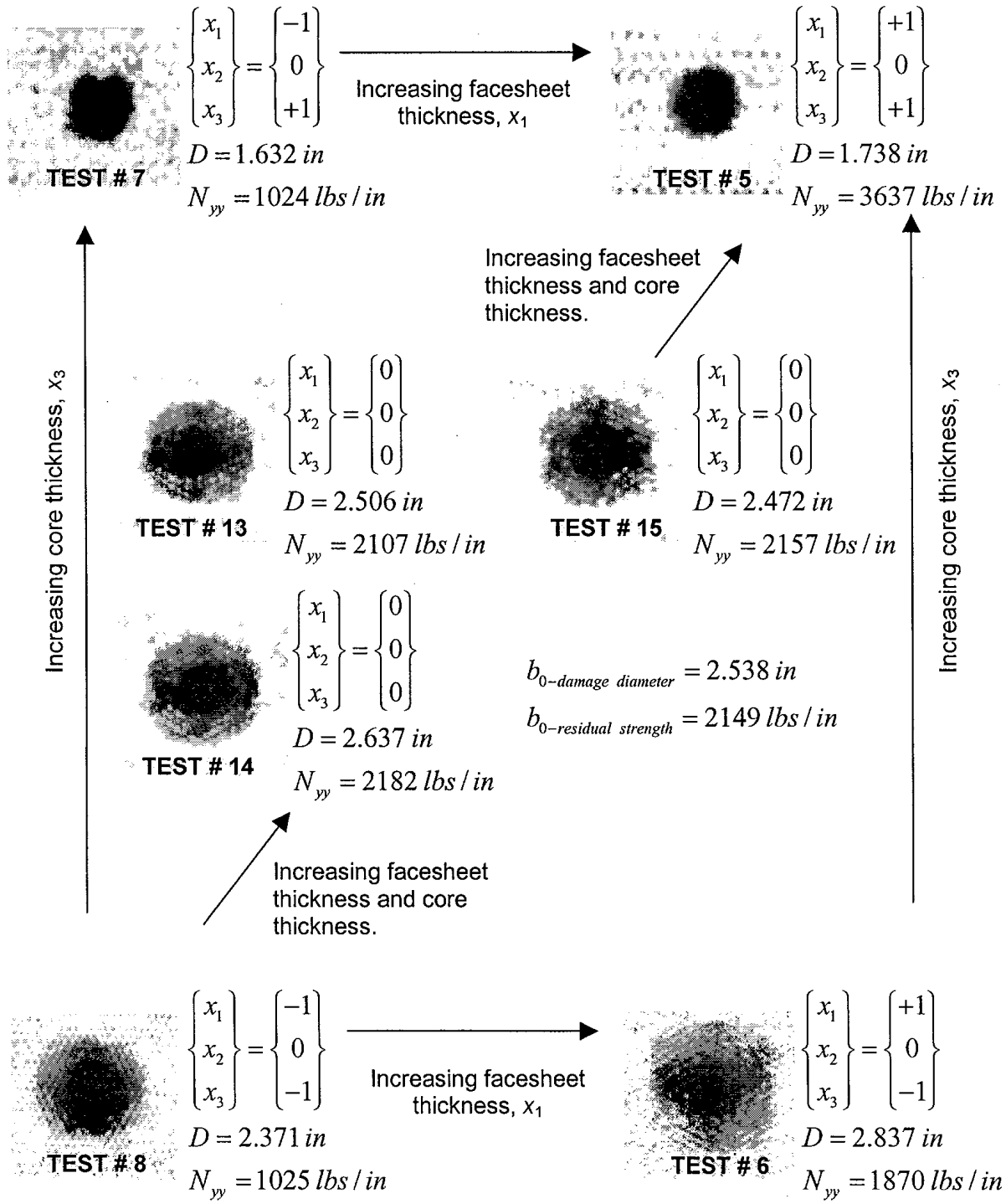

FIGURE 7. MEASURED DAMAGE DIAMETER [13] AND RESIDUAL STRENGTH FOR CORE DENSITY, X_2 = 4.5 lbs/ft^3 ($x_2 = 0$)

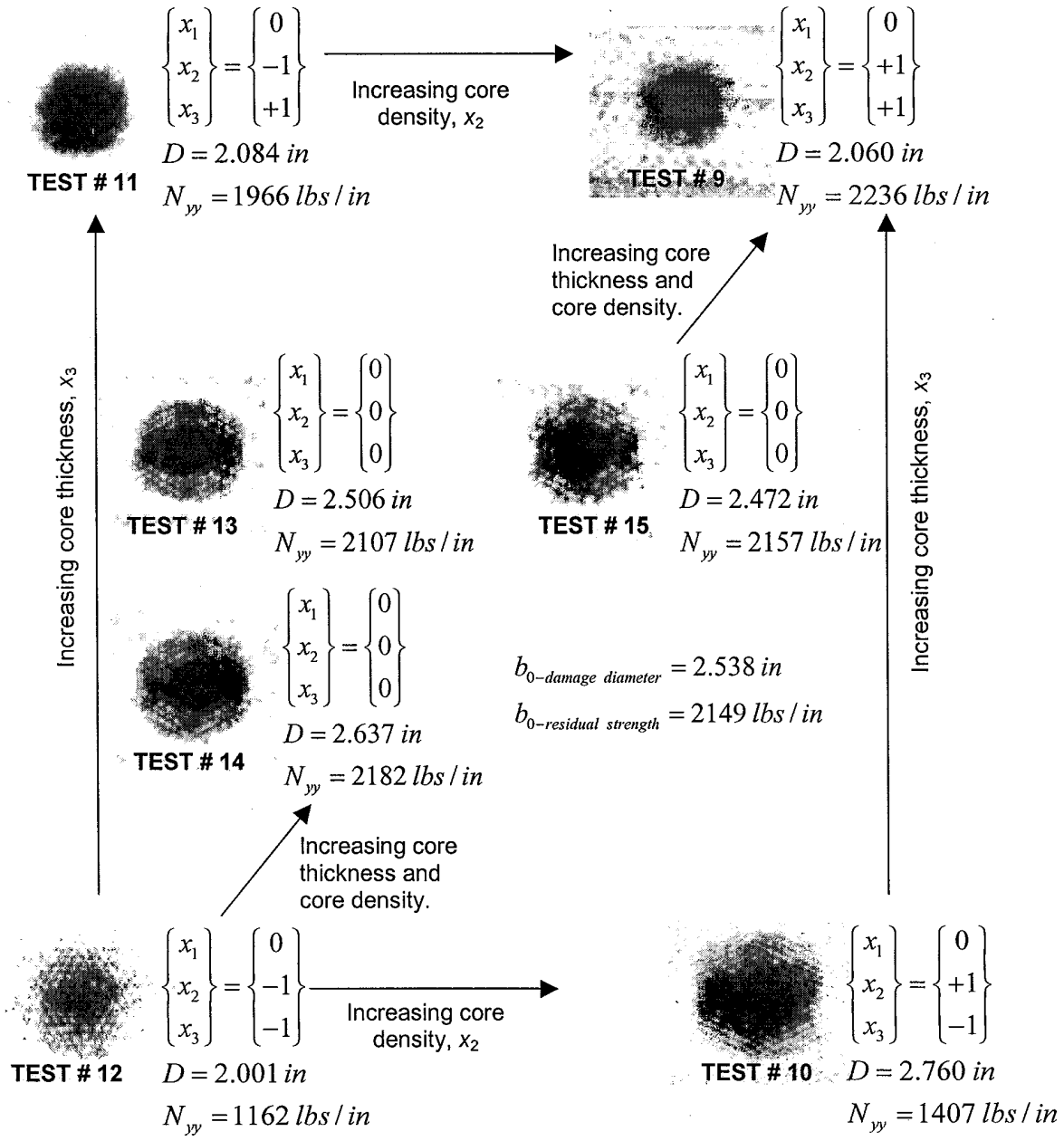

FIGURE 8. MEASURED DAMAGE DIAMETER [13] AND RESIDUAL STRENGTH FOR FACESHEET CONFIGURATION, X_1 = 4 plies $[90/45]_2$ (x_1 = 0)

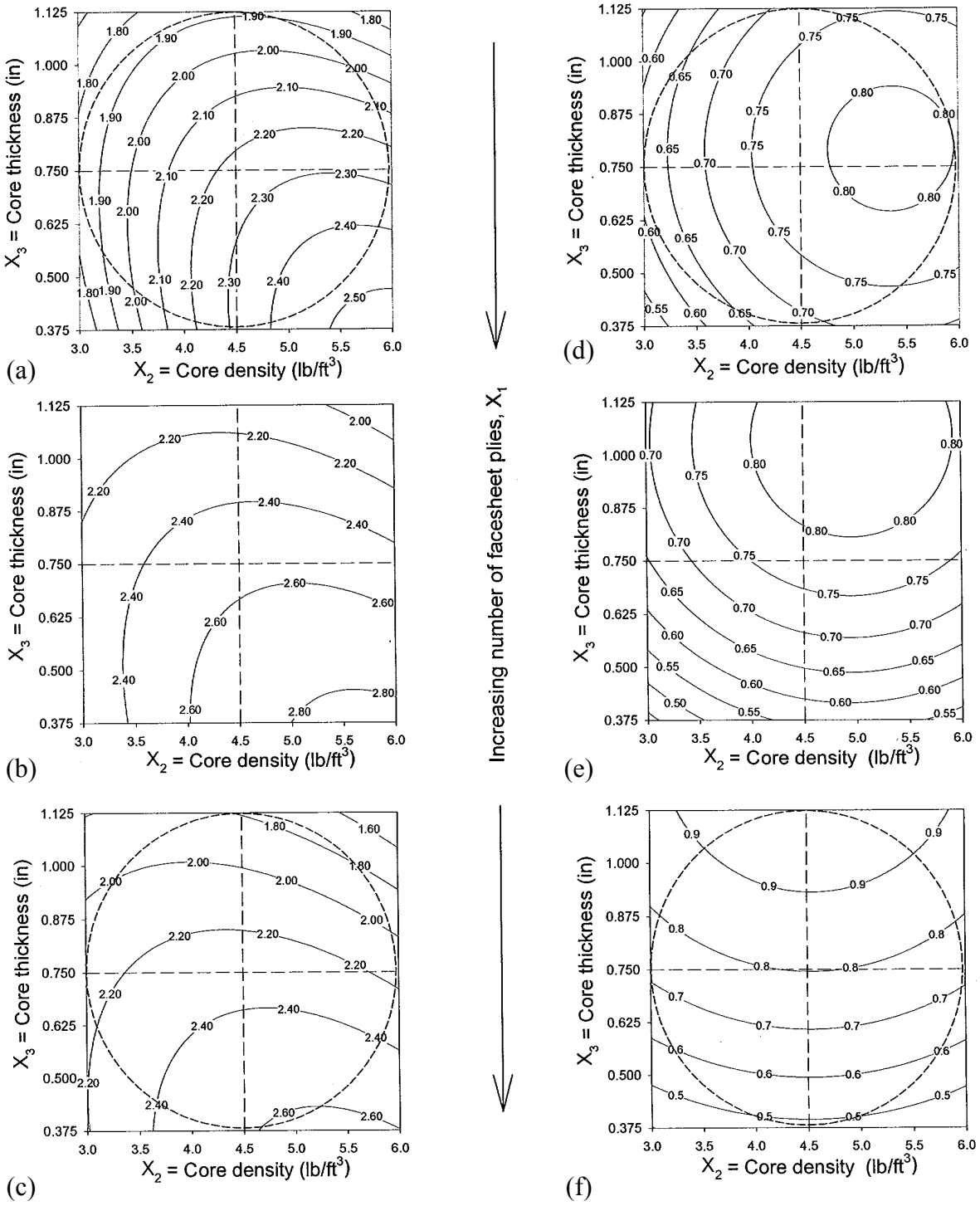

FIGURE 9. PREDICTED DAMAGE DIAMETER (in) FOR X_1: (a) TWO, (b) FOUR, AND (c) SIX PLIES [13]; PREDICTED NORMALIZED RESIDUAL STRENGTH FOR X_1: (d) TWO, (e) FOUR, AND (f) SIX PLIES

A comparison of figures 9(d), 9(e), and 9(f) suggests that the given impact can result in residual strength values that range roughly between 50%-90% of the virgin panel strength for a given facesheet configuration. Response surfaces similar to equation 8 may allow manufacturers to estimate the peak degradation in CAI residual strength for a given class of impact (i.e., establish conservative knockdown factors to the virgin panel strength that arguably account the influence of expected impacts). Such information may prove valuable in the initial design and sizing of key sandwich composite structural components as well as in the specification of design allowables for damage tolerant parts. Special care must be taken to ensure that the range of impact variables (impactor diameter, impact energy, impact velocity, etc.) used in the development represent a realistic threat to a given structural element.

Table 4 contains a limited set of additional independent experimental results from Tomblin et al. [5], where the combination of sandwich configuration variables (X_1, X_2, X_3) = (4 plies, 3.0 lb/ft^3, 3/4 in) or (x_1, x_2, x_3) = (0, -1, 0) lie within a coded radius, $r = \sqrt{2} = 1.414$, of the center point of the experimental design. Response surface predictions of the planar diameter, $\hat{D}$, of the internal damage from reference 13 are compared to the measured diameter, D, and the CAI residual strength (equation 7) are compared to measured residual strengths in table 4. Note that response surface estimates for predicted CAI residual strength using equation 7 more closely matched the limited experimental results than response surface estimates of the TTU C-scan diameter from reference 13. This is consistent with scatter observed in figure 3. The mean value of the experimentally CAI residual strengths (N_{yymean} = 1792 lbs/in) for this sandwich panel configuration differed from the value predicted in equation 7 by 3.5%. The difference between individual measurements and the predicted value varied between 3.7% and 8.7%, with a mean difference of 5.9%. This suggests that response surfaces similar to equation 7 may be useful tools in identifying combinations of sandwich composite parameters leading to improved damage tolerance properties for a given class of impact.

TABLE 4. INTERPOLATION OF REGRESSION RESULTS IN THE SPACE OF CODED MATERIAL VARIABLES

x_1	x_2	x_3	r	Measured Damage Diameter, D (in) [13]	Predicted Damage Diameter, $\hat{D}$ (in) [13]	$\left\|\frac{D-\hat{D}}{D}\right\|$ (%)	Measured Residual Strength, N_{yy} (lbs/in)	Predicted Residual Strength, $\hat{N}_{yy}$ (lbs/in)	$\left\|\frac{N_{yy}-\hat{N}_{yy}}{N_{yy}}\right\|$ (%)
0	-1	0	1	2.046	2.239	9.4	1736	1855	6.9
0	-1	0	1	2.131	2.239	5.1	1935	1855	4.1
0	-1	0	1	2.056	2.239	8.9	1790	1855	3.7
0	-1	0	1	2.851	2.239	21.5	1708	1855	8.7

2.2 INFLUENCE OF FACESHEET THICKNESS, IMPACT ENERGY, AND IMPACTOR DIAMETER ON THE IMPACT DAMAGE TOLERANCE OF SANDWICH COMPOSITES.

In the preceding section, the isolated influence of sandwich configuration parameters on the damage tolerance properties of sandwich composites was investigated for a fixed set of impact parameters. In this study, the isolated effects of the number of facesheet plies (X_1), impact energy (X_4), and impactor diameter (X_5) on the damage tolerance characteristics of sandwich composite panels were investigated using the Box-Behnken experimental design. Lacy et al. [13] conducted a similar study investigating the influence of these parameters on the damage resistance characteristics of sandwich composites for the same set of test specimens considered here. Table 5 summarizes the low, midrange, and high levels of the natural (X_1, X_4, X_5) and coded (x_1, x_4, x_5) independent variables considered in this examination. Here, the core density ($X_2 = 3.0$ lb/ft^3), core thickness ($X_3 =$ 3/4 in), and impact velocity ($X_6 =$ 96.3 in/s) were held fixed.

TABLE 5. NATURAL VALUES AND CORRESPONDING CODED LEVELS OF THE FACESHEET PLIES AND IMPACT VARIABLES

i	Independent Variable	Natural Value, X_i	Coded Level, x_i
1	Number of Facesheet Plies	2 $[90/45]_1$	-1
		4 $[90/45]_2$	0
		6 $[90/45]_3$	+1
4	Impact Energy	90.0 in-lbs	-1
		120.0 in-lbs	0
		150.0 in-lbs	+1
5	Impactor Diameter	1.0 in	-1
		2.0 in	0
		3.0 in	+1

Table 6 summarizes the combinations of coded independent variables as well as the experimentally measured residual strengths for the 15 experiments used in the regression analysis. Following a procedure similar to that used to develop the response surfaces (equation 7 and 8), statistically reliable, second-order response surfaces were generated that characterize the CAI residual strength as a continuous function of the number of facesheet plies, impact energy, and impactor diameter. It is especially important to consider the possibility of bifurcations between failure modes when interpreting the regression results. An estimate of the CAI residual strength from the regression analysis may be expressed either in terms of coded or natural values of the independent variables, i.e.,

$$\begin{aligned}\hat{N}_{yy} &= 1722 + 733.0 \cdot x_1 - 225.2 \cdot x_4 - 35.57 \cdot x_5 \\ &\ldots - 134.0 \cdot x_1^2 + 29.57 \cdot x_4^2 - 177.1 \cdot x_5^2 \qquad \text{(lbs/in)} \qquad (9a) \\ &\ldots - 221.0 \cdot x_1 \cdot x_4 - 161.6 \cdot x_1 \cdot x_5 - 72.47 \cdot x_4 \cdot x_5\end{aligned}$$

and

$$\hat{N}_{yy} = -2537 + 1238 \cdot X_1 + 4.176 \cdot X_4 + 1286 \cdot X_5$$
$$\ldots - 33.50 \cdot X_1^2 + 0.033 \cdot X_4^2 - 177.1 \cdot X_5^2 \qquad \text{(lbs/in)} \qquad (9b)$$
$$\ldots - 3.684 \cdot X_1 \cdot X_4 - 80.78 \cdot X_1 \cdot X_5 - 2.416 \cdot X_4 \cdot X_5$$

TABLE 6. COMPARISONS BETWEEN PREDICTED AND MEASURED RESIDUAL STRENGTH

Test, k	x_1	x_4	x_5	Measured Residual Strength, N_{yy} (lbs/in)	Predicted Residual Strength, $\hat{N}_{yy}$ (lbs/in)	$\left\lvert \frac{N_{yy} - \hat{N}_{yy}}{N_{yy}} \right\rvert$ (%)
16	+1	+1	0	1913	1905	0.4
17	+1	-1	0	2942	2797	4.9
18	-1	+1	0	735.5	880.7	19.7
19	-1	-1	0	880.5	889	1.0
20	+1	0	+1	1811	1947	7.5
21	+1	0	-1	2323	2341	0.8
22	-1	0	+1	822.1	804.2	2.2
23	-1	0	-1	688.0	552.2	19.7
24	0	+1	+1	1369	1242	9.3
25	0	+1	-1	1467	1458	0.6
26	0	-1	+1	1827	1837	0.5
27	0	-1	-1	1636	1763	7.8
28	0	0	0	1666	1722	3.4
29	0	0	0	1712	1722	0.6
30	0	0	0	1789	1722	3.7

The constant term (b_0 = 1722 lbs/in) in equation 9a represents the mean CAI residual strength for those panels corresponding to the center point of the design. Based upon the magnitudes of the coefficients of the linear terms in equation 9a, the coded number of facesheet plies, x_1, and impact energy, x_4, contribute the most to the linear variation in the predicted response at points removed from the center point (x_1, x_4, x_5) = (0, 0, 0) of the designed test matrix. As might be expected, increasing the number of facesheet plies and/or decreasing the impact energy and impactor diameter will result in a linear increase in the estimated CAI strength from b_0. Lacy et al. [13] noted that increasing either the impact energy or the impactor diameter will generally produce internal damage that is spread over a greater area. Similar arguments can be made when interpreting the influence of the remaining quadratic and coupling terms in equation 9a on the predicted response.

2.2.1 Discussion of Facesheet Plies and Impact Parameter Regression Model Results.

Table 6 summarizes the measured and predicted CAI residual strength for each of the sandwich composite panels considered in this effort. The difference between the experimentally measured residual strengths and the estimated values using equation 9 varied between 0.4% and 19.7% for the 15 panels tested, with a mean difference of 5.5%. This suggests that the response surface (equation 9) may provide a reasonable characterization of the influence of the number facesheet plies, impact energy, and impactor diameter on the CAI residual strength if the number of facesheet plies is greater than two. The regression results may also be viewed schematically in the space of coded independent variables, as shown in figure 10. Similar to the previous results (cf., table 3), the differences between the observed and predicted residual strengths were greatest for those sandwich panels with two-ply facesheets (~20% disparity). Recall that sandwich panels comprised of thinner facesheets are somewhat more susceptible to failure in compression due to facesheet fracture, since the relative lack of bending rigidity in the individual facesheets may impede the onset of progressive dimple propagation. The likelihood of facesheet fracture may be exacerbated by any stress concentration due to varied facesheet damage. As the number of facesheet plies is reduced, and the possibility of facesheet penetration increases, there is a transition in failure mode from predominately progressive dimple propagation to facesheet fracture. This may explain why the regression results do not more closely correlate with the experimental observations for panels with two-ply facesheets.

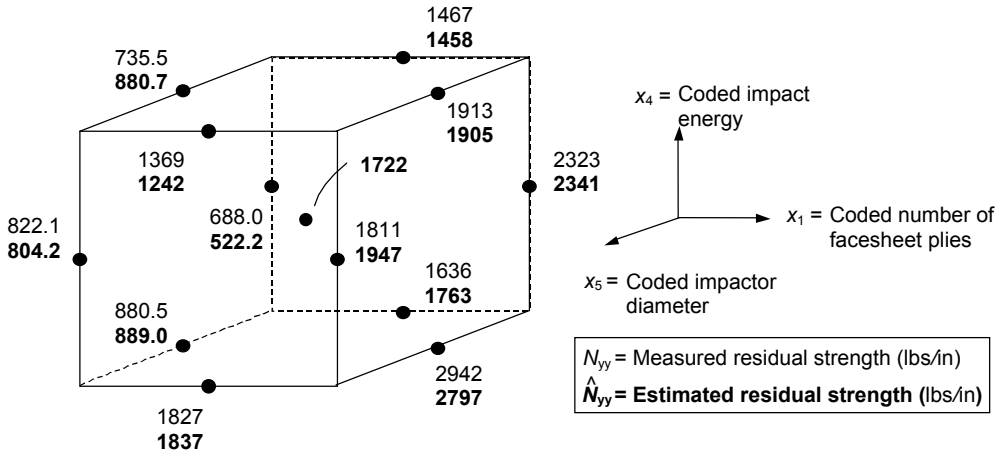

FIGURE 10. RESPONSE SURFACE ESTIMATES OF RESIDUAL STRENGTH AS A FUNCTION OF FACESHEET PLIES AND IMPACT PARAMETERS

Figure 11 summarizes the influence of the number of facesheet plies (X_1, x_1), impact energy (X_4, x_4), and impactor diameter (X_5, x_5) on the estimate of CAI residual strength (equation 9). Figures 11(a), 11(b), and 11(c) show the CAI residual strength (equation 9) as a function of impact energy and impactor diameter for the two-ply, four-ply, and six-ply facesheet configurations (or x_1 = -1, 0, 1), respectively. Similar to the results from the previous section, a comparison of the three figures reveals that the predicted strength increases substantially as the number of facesheet plies is increased. For the two-ply facesheet configuration (figure 11(a)),

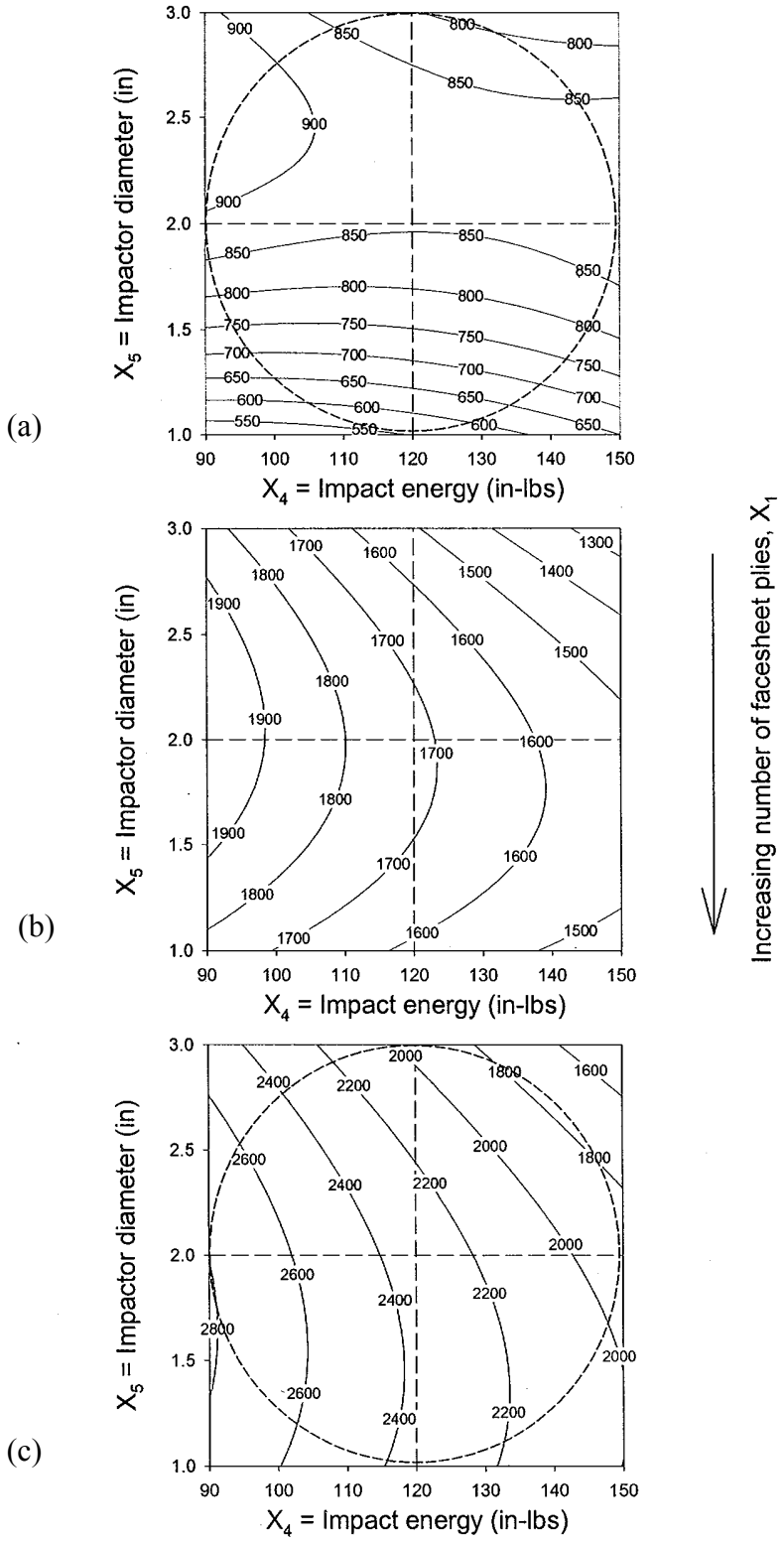

FIGURE 11. PREDICTED RESIDUAL STRENGTH (lbs/in): (a) X_1 = 2 plies $[90/45]_1$, (b) X_1 = 4 plies $[90/45]_2$, AND (c) X_1 = 6 plies $[90/45]_3$

the estimated CAI strength generally increases with increasing impactor diameter and is somewhat insensitive to the impact energy level. One possible explanation for the increase in the estimated strength is that as the diameter of the impactor is increased and the potential for facesheet penetration is reduced, more load may be transferred across the impact site. The compressive failure mechanisms and residual strength are likely influenced by whether or not partial facesheet penetration occurs. This is of particular concern for those impacts involving smaller diameter impactors and/or increasing impact energy. For the four-ply and six-ply facesheet configurations (figures 11(b) and 11(c)), which have somewhat higher penetration resistance and bending rigidity, the estimated strength is a generally decreasing function of impact energy. For the four-ply facesheet configuration, there is additional damage for small diameter impactors that reduces the residual strength. At midrange-to-high impact energy levels, the predicted response is a decreasing function of impactor diameter, particularly for the six-ply facesheet configuration; increasing the impactor diameter from 2.0 in to 3.0 in OD can result in a significant reduction in the estimated CAI strength (figure 11(c)). For specimens with thicker facesheets, widespread core damage resulting from impacts involving larger diameter impactors may promote CAI failure due to progressive facesheet dimple propagation. Small diameter impactors seem to introduce other damage mechanisms. This underscores the need to consider a variety of impactor diameters when establishing a damage tolerance plan for sandwich composite aircraft structures.

The preceding results are in agreement with the experimental observations. Figures 12 through 14 show the recorded CAI residual strengths for the test specimens corresponding to the midrange impactor diameter ($x_5 = 0$; $X_5 = 2$ in), midrange impact energy ($x_4 = 0$; $X_4 = 120$ in-lbs), and midrange facesheet configurations ($x_1 = 0$; $X_1 = 4$ plies), respectively. Included with each observation is its associated TTU C-scan image and measured diameter, D, from reference 13. These figures suggest that the experimentally observed CAI strengths for a given facesheet configuration are consistent with the regressions of figure 11. Again, the observed CAI strengths for the four-ply and six-ply facesheet configurations generally were inversely proportional to the diameter of the TTU C-scan images reported in reference 13.

For the test matrix summarized in table 6, figure 15 contains a comparison of the response surface predictions of the TTU C-scan diameter from reference 13 to the response surface predictions of the normalized CAI residual strength developed in this examination. Comparing figures 15(a), 15(b), and 15(c) to figures 15(d), 15(e), and 15(f), respectively, shows that, with the exception of the two-ply facesheet configuration (figures 15(a) and 15(d) and four-ply facesheet configurations under low-impact energy and small impactor diameters (figures 15(b) and 15(e)), the maximum degradation in residual strength and the maximum TTU C-scan diameter both correspond to higher-energy impacts involving 3.0 in OD impactors. This is consistent with the observations of Tomblin et al. [5] (cf., figure 2). Again, for impacts involving partial facesheet penetration, there may be no clear correlation between the measured TTU C-scan diameter and CAI residual strength. A comparison of figures 15(d), 15(e), and 15(f) suggests that the CAI residual strength can range roughly between 45%-70% of the virgin panel strength for a given facesheet configuration. Similar to the results shown in figure 11, the estimated normalized residual strength for the four-ply and six-ply facesheet configurations may decrease significantly with increasing impact energy and impactor diameter.

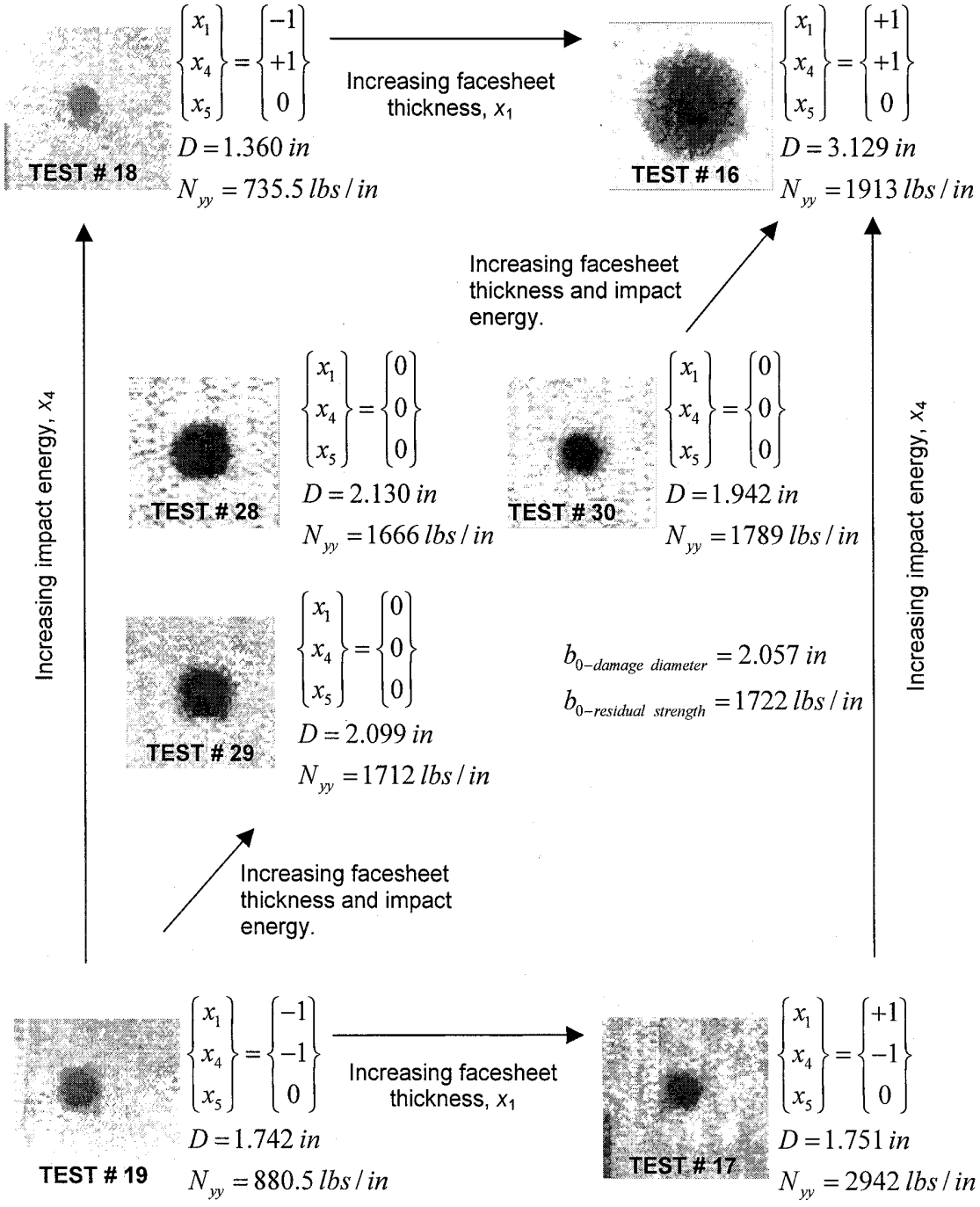

FIGURE 12. MEASURED DAMAGE DIAMETER [13] AND RESIDUAL STRENGTH FOR IMPACTOR DIAMETER, X_5 = 2.00 in (x_5 = 0)

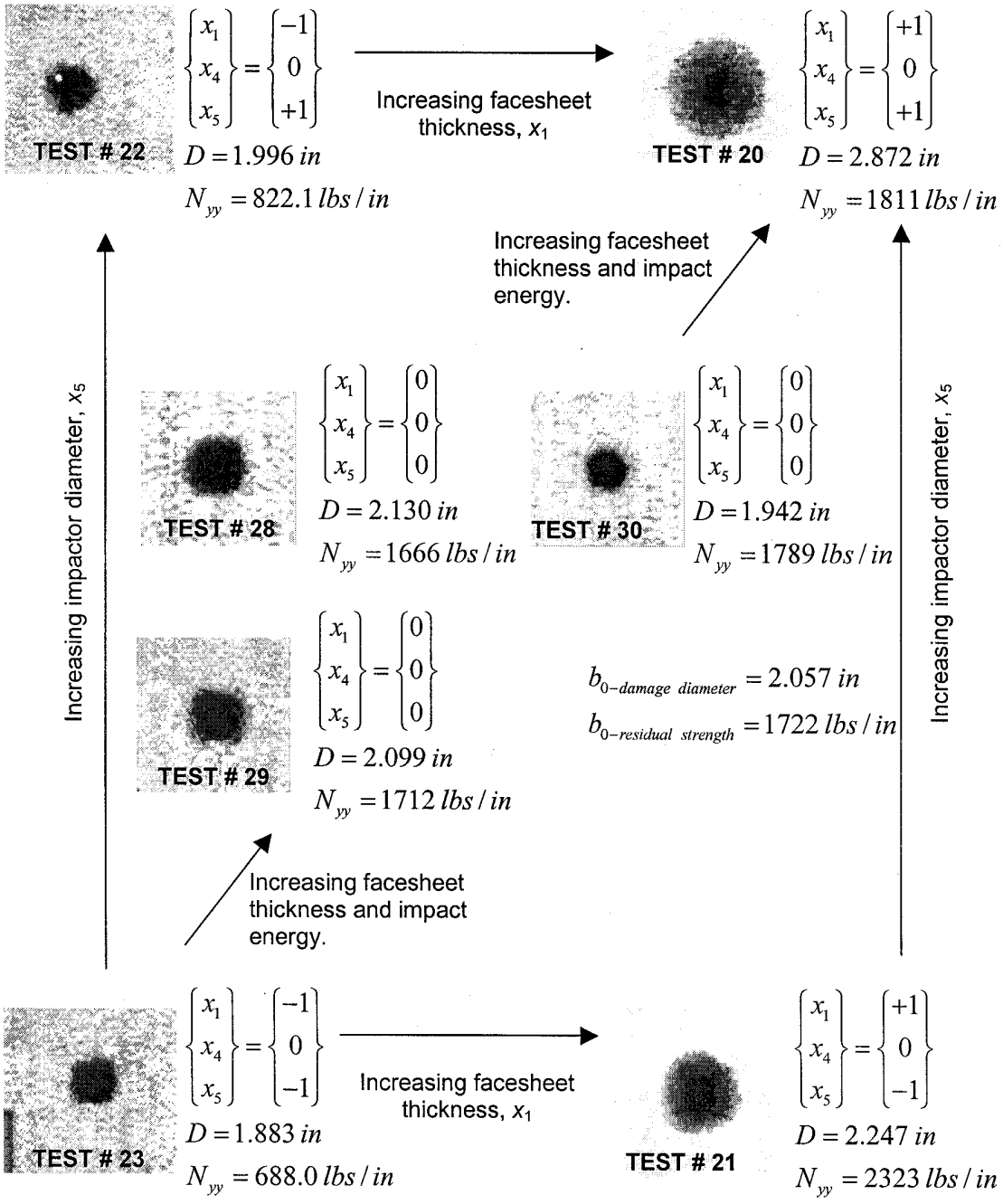

FIGURE 13. MEASURED DAMAGE DIAMETER [13] AND RESIDUAL STRENGTH FOR IMPACT ENERGY, X_4 = 120 in-lbs (x_4 = 0)

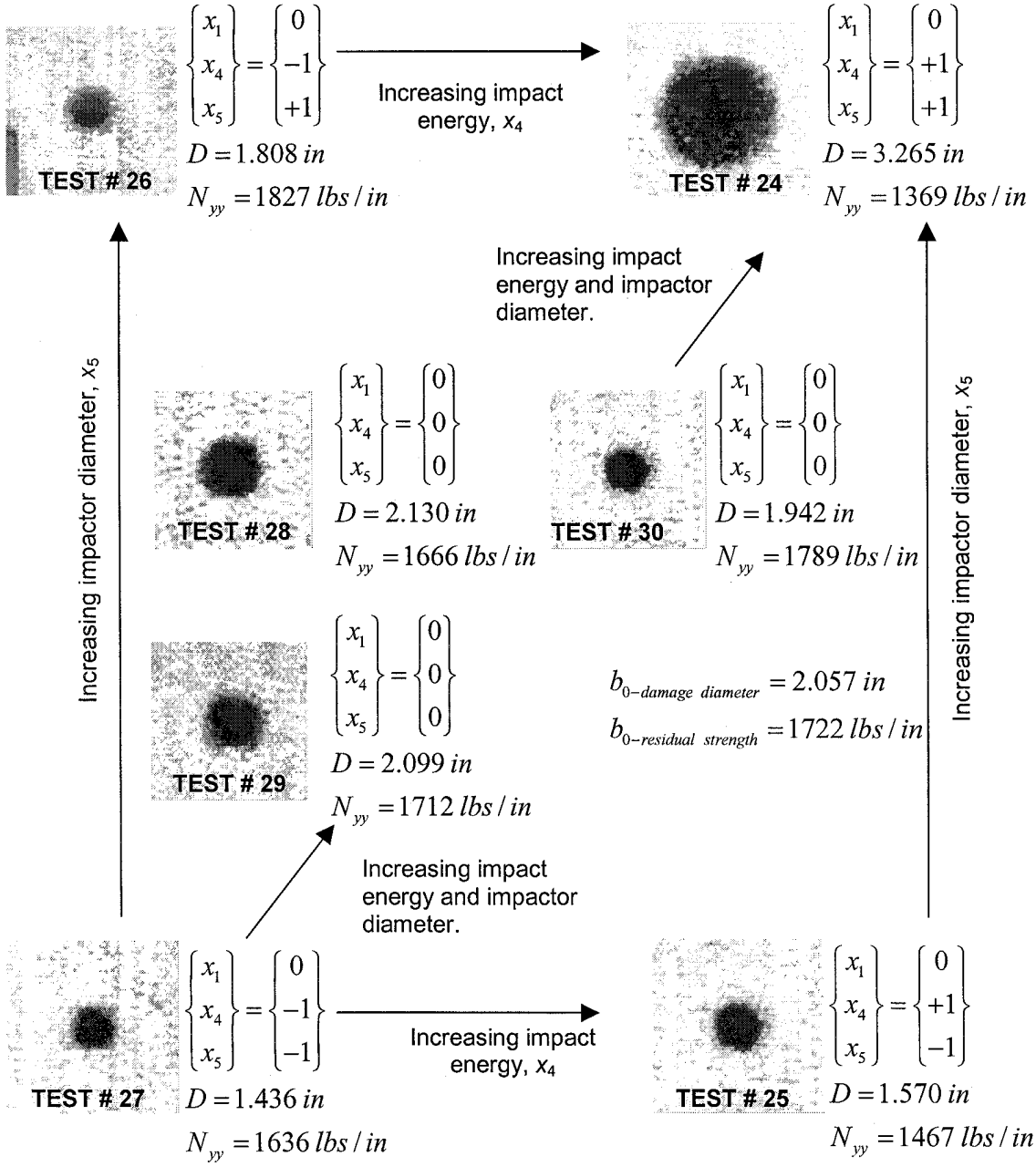

FIGURE 14. MEASURED DAMAGE DIAMETER [13] AND RESIDUAL STRENGTH FOR FACESHEET CONFIGURATION, $X_1 = 4$ plies $[90/45]_2$ ($x_1 = 0$)

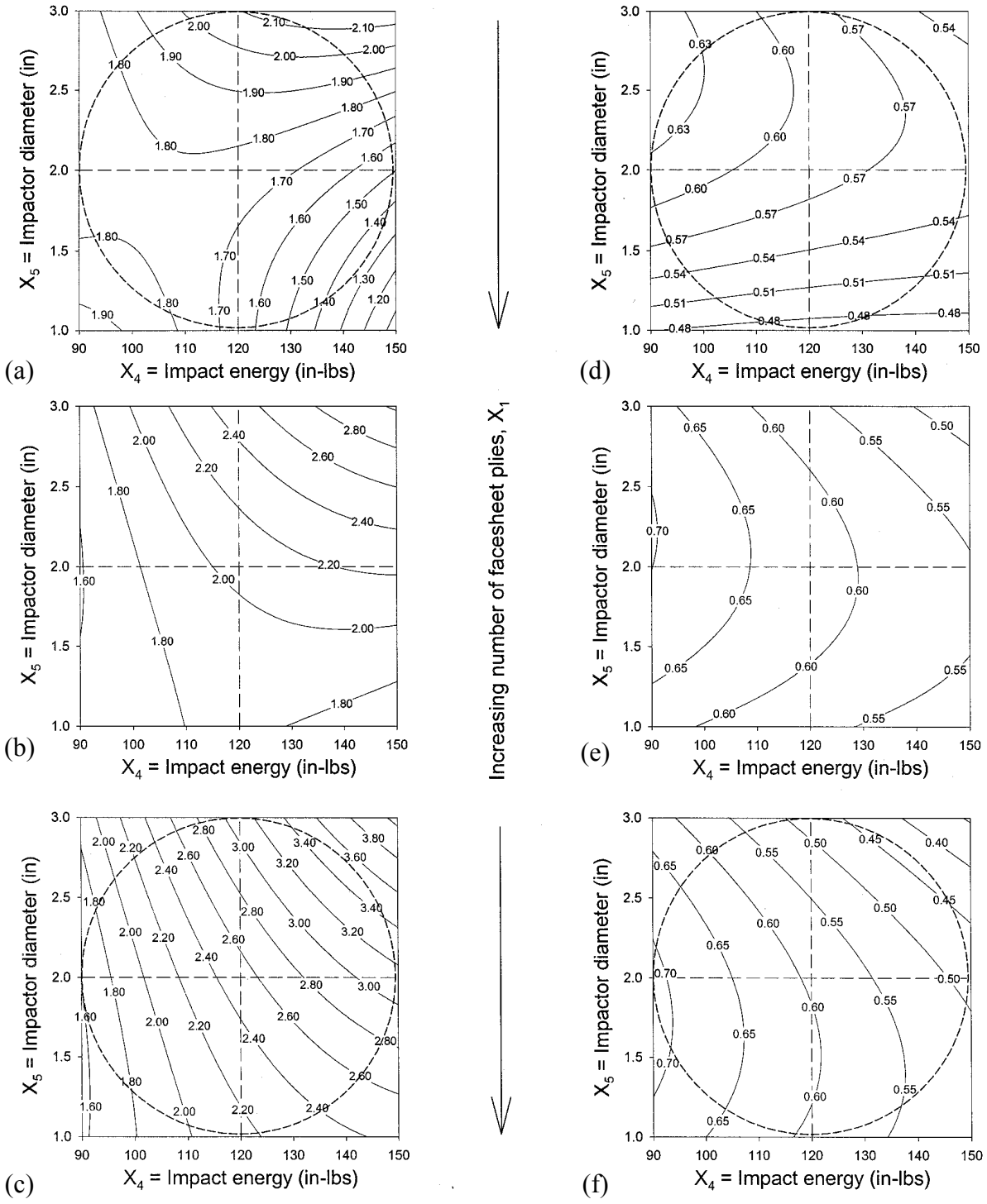

FIGURE 15. PREDICTED DAMAGE DIAMETER (in) FOR X_1: (a) TWO, (b) FOUR, AND (c) SIX PLIES [13]; PREDICTED NORMALIZED RESIDUAL STRENGTH FOR X_1: (d) TWO, (e) FOUR, AND (f) SIX PLIES

2.2.2 Correlation With Independent Experimental Results.

Table 7 contains a set of additional independent experimental results from Tomblin et al. [5], where the ranges of coded material system and impact variables are in the vicinity of those considered in this study. Response surface predictions of the planar diameter, $\hat{D}$, of the internal damage from reference 13 are compared to measured damage diameters, D, from reference 13. Also shown in table 7 are the measured and the predicted (using equation 9) CAI residual strengths. Note that the predicted errors for CAI residual strength using equation 9 are comparable to those for the damage diameter from reference 13. The combinations of the coded number of facesheet plies (x_1), impact energy (x_4), and impactor diameter (x_5), contained in the first eight rows of the table lie within a coded radius, $r = \sqrt{2} = 1.414$, of the center point of the experimental design; interpolation of response surface results is appropriate for these data. The remaining combinations of independent variables correspond to $r > \sqrt{2}$. Using the response surface (equation 9) for the latter case corresponds to an extrapolation beyond the range of independent variables used in the regression; such estimates are denoted in the table by an asterisk (*). The difference between the experimentally measured CAI residual strengths and the interpolated values varied between 1.7% and 22.6%, with a mean difference of 14.0%. Hence, the response surface estimates using equation 9 correlate moderately well with the experimental data within the space of the Box-Behnken design. The first three extrapolated values of the strength contained in the table correspond to combinations of independent variables that fall just outside of the coded radius, $r = \sqrt{2}$; the response surface estimates (equation 9) correlate reasonably well with the experimental data for these cases. The remaining combinations of independent variables, however, correspond to extrapolation of regression results toward various corners of the cube shown in figure 10 (i.e., $r = \sqrt{x_1^2 + x_4^2 + x_5^2} \approx \sqrt{3} = 1.732$).

Table 7 shows the magnitudes of the differences between measured and extrapolated values of the CAI residual strength that can be significantly larger than for the case involving interpolation of results. The maximum difference between the measured and extrapolated results (46.6%) occurred for (x_1, x_4, x_5) = (-1, -0.95, -1) or (X_1, X_4, X_5) = (2 plies, 91.5 in-lbs, 1.0 in). Figure 11(a) shows that a relatively large gradient exists in the extrapolated response surface prediction along the radial line defined by the points (X_1, X_4, X_5) = (2 plies, 120.0 in-lbs, 2.0 in) and (X_1, X_4, X_5) = (2 plies, 90.0 in-lbs, 1.0 in). Clearly, extreme caution must be used to ensure that response surfaces estimates are only evaluated in the spherical domain associated with the experimental design (in this case, $r \le \sqrt{2}$). In addition, the range in the number of facesheet plies, impact energies, and impactor diameters considered in this study increase the probability of a bifurcation in failure modes. This may explain why the response surface (equation 9) did not perform as well in comparison to independent experimental data as did the response surface (equation 7) developed in the previous section for the case where the impact energy and impactor diameter were held fixed. It should be noted that the response surfaces generally underpredict the residual strength and overpredict the damage diameter.

TABLE 7. INTERPOLATION AND EXTRAPOLATION* OF REGRESSION RESULTS IN THE SPACE OF CODED MATERIAL AND IMPACT VARIABLES

x_1	x_4	x_5	R	Measured Damage Diameter, D (in) [13]	Predicted Damage Diameter, $\hat{D}$ (in) [13]	Prediction Errors $\left\|\frac{D-\hat{D}}{D}\right\|$ (%)	Measured Residual Strength, N_{yy} (lbs/in)	Predicted Residual Strength, $\hat{N}_{yy}$ (lbs/in)	Prediction Errors $\left\|\frac{N_{yy}-\hat{N}_{yy}}{N_{yy}}\right\|$ (%)
0	0.03	-1	1.000	1.898	1.815	4.4	1603	1576	1.7
0	0.04	1	1.001	2.046	2.541	24.2	1736	1498	13.7
0	0.04	1	1.001	2.131	2.541	19.3	1935	1498	22.6
0	0.05	1	1.001	2.056	2.551	23.9	1790	1493	16.6
0	0.28	-1	1.038	1.641	1.802	9.8	1894	1540	18.7
0	0.30	1	1.044	2.851	2.698	5.3	1708	1424	16.6
0	0.76	1	1.256	2.531	2.927	15.7	N/A	N/A	N/A
0	-0.98	1	1.400	2.022	1.739	14.1	1985	1828	7.9
0	-1.01	-1	1.421*	1.603	1.673*	4.4*	1894	1766*	6.8*
-1	0.19	1	1.427*	2.281	2.130*	6.6*	787	790*	0.5*
-1	0.22	1	1.431*	2.485	2.134*	14.1*	834	789*	5.4*
-1	-0.73	1	1.592*	2.283	1.862*	18.5*	846	876*	3.5*
-1	-0.77	-1	1.610*	1.421	1.908*	34.3*	880	517*	41.2*
1	0.78	1	1.615*	2.254	3.867*	71.7*	2690	1562*	41.9*
1	-0.86	1	1.655*	2.291	2.055*	10.2*	2453	2416*	1.5*
-1	-0.95	-1	1.704*	1.578	1.944*	23.1*	964	514*	46.6*
-1	0.97	1	1.715*	2.594	2.165*	16.5*	848	758*	10.6*
1	-1.06	1	1.767*	1.724	1.784*	3.4*	3143	2529*	19.6*
1	-1.12	-1	1.804*	1.530	1.483*	3.2*	2840	2796*	1.6*
-1	-1.17	1	1.835*	1.872	1.646*	12.1*	825	934*	13.2*

()* = Extrapolated values

2.3 INFLUENCE OF FACESHEET THICKNESS, IMPACT ENERGY, AND IMPACT VELOCITY ON THE IMPACT DAMAGE TOLERANCE OF SANDWICH COMPOSITES.

In the final study in this examination, the isolated effects of the number of facesheet plies (X_1), impact energy (X_4), and impact velocity (X_6) on the damage tolerance characteristics of sandwich composite panels were investigated using the Box-Behnken experimental design. Here, different impact velocities resulting in a particular value of impact energy were obtained by varying the impactor mass and drop height during the impact testing (cf., [5]). The influence of dynamic effects on the damage tolerance properties of the given sandwich composites over a range of relatively low-velocity impacts is being studied. Table 8 summarizes the low, midrange, and high levels of the natural (X_1, X_4, X_6) and coded (x_1, x_4, x_6) independent variables considered in this effort. The core density (X_2 = 3.0 lb/ft^3), core thickness (X_3 = 3/4 in), and impactor diameter (X_5 = 3.0 in) were held fixed.

TABLE 8. NATURAL VALUES AND CORRESPONDING CODED LEVELS OF THE FACESHEET THICKNESS AND IMPACT VARIABLES

i	Independent Variable	Natural Value, X_i	Coded Level, x_i
1	Number of Facesheet Plies	2 $[90/45]_1$	-1
		4 $[90/45]_2$	0
		6 $[90/45]_3$	+1
4	Impact Energy	90.0 in-lbs	-1
		120.0 in-lbs	0
		150.0 in-lbs	+1
6	Impact Velocity	65.21 in/s	-1
		96.30 in/s	0
		127.39 in/s	+1

Table 9 summarizes the combinations of coded independent variables as well as the experimentally measured CAI strengths for the 15 experiments used in the regression analysis. Following the procedure outlined earlier, statistically reliable, second-order response surfaces were generated that characterize the CAI residual strength as a continuous function of the number of facesheet plies, impact energy, and impact velocity. An estimate of the CAI residual strength from the regression analysis may be expressed either in terms of coded or natural values of the independent variables, i.e.,

$$\begin{aligned}\hat{N}_{yy} &= 1820 + 776.9 \cdot x_1 - 135.65 \cdot x_4 - 4.930 \cdot x_6 \\ &\ldots - 97.67 \cdot x_1^2 + 153.9 \cdot x_4^2 - 398.9 \cdot x_6^2 \qquad \text{(lbs/in)} \\ &\ldots - 119.0 \cdot x_1 \cdot x_4 - 20.09 \cdot x_1 \cdot x_6 + 21.65 \cdot x_4 \cdot x_6\end{aligned} \tag{10a}$$

and

$$\begin{aligned}\hat{N}_{yy} &= -1740 + 853.0 \cdot X_1 - 39.86 \cdot X_4 + 77.83 \cdot X_6 \\ &\ldots - 24.42 \cdot X_1^2 + 0.1710 \cdot X_4^2 - 0.4127 \cdot X_6^2 \qquad \text{(lbs/in)} \\ &\ldots - 1.984 \cdot X_1 \cdot X_4 - 0.3231 \cdot X_1 \cdot X_6 + 0.0232 \cdot X_4 \cdot X_6\end{aligned} \tag{10b}$$

The constant term (b_0 = 1820 lbs/in) in equation 10a represents the mean CAI residual strength for those panels corresponding to the center point of the design. Consistent with earlier observations, increasing the number of facesheet plies, x_1, from their midrange value in equation 10a will result in a linear increase in the predicted response, whereas increasing the impact energy, x_4, and impact velocity, x_6, will result in a somewhat smaller linear decrease in the estimated residual strength from b_0. Note that the quadratic term involving the impact velocity contributes significantly to the estimated response (i.e., the midrange velocity likely defines a relative maximum or ridge in the predicted response). Similar arguments can be made when interpreting the influence of the remaining quadratic and coupling terms in equation 10a on the estimated residual strength.

TABLE 9. COMPARISONS BETWEEN PREDICTED AND MEASURED RESIDUAL STRENGTH

Test, k	x_1	x_4	x_6	Measured Residual Strength, N_{yy} (lbs/in)	Predicted Residual Strength, $\hat{N}_{yy}$ (lbs/in)	$\left\|\frac{N_{yy}-\hat{N}_{yy}}{N_{yy}}\right\|$ (%)
31	+1	+1	0	2690	2399	10.8
32	+1	-1	0	3143	2908	7.5
33	-1	+1	0	847.8	1083	27.8
34	-1	-1	0	824.9	1116	35.3
35	+1	0	+1	1774	2076	17.0
36	+1	0	-1	1901	2126	11.8
37	-1	0	+1	786.7	562.1	28.6
38	-1	0	-1	833.8	531.7	36.2
39	0	+1	+1	1467	1456	0.7
40	0	+1	-1	1356	1423	4.9
41	0	-1	+1	1751	1684	3.8
42	0	-1	-1	1727	1738	0.6
43	0	0	0	1935	1820	5.9
44	0	0	0	1736	1820	4.8
45	0	0	0	1790	1820	1.7

2.3.1 Discussion of Facesheet Thickness and Impact Parameter Regression Model Results.

Table 9 summarizes the measured and predicted CAI strength for each of the sandwich composite panels. The difference between the experimentally measured CAI residual strengths and the estimated values using equation 10 varied between 0.2% and 36.2% for the 15 panels tested, with a mean difference of 13.2%. The lack of correlation was especially pronounced for x_1 = -1 (X_1 = 2 plies). A comparison of the data from tables 3, 6, and 9 considered in the development of the response surfaces (equations 7, 9, and 10), respectively, suggests that those specimens with two-ply facesheet configurations often showed the biggest disparity between the measured and estimated CAI residual strengths. As mentioned previously, the compressive failure mechanisms (facesheet fracture, facesheet dimple propagation, etc.) and residual strength are likely influenced by whether or not partial facesheet penetration occurs; the nature and severity of the local damage also may be drastically different for the two cases. This is of particular concern for those impacts involving smaller diameter impactors, increasing impact energy, and/or thinner facesheets. Quadratic response surfaces, such as equation 10, have difficulty predicting the CAI strength for those test panel configurations exhibiting a bifurcation between failure modes over the range of input parameters considered. Hence, the response surface estimate (equation 10) is likely inaccurate for the class of blunt object impacts considered here. Qualitative consideration of the response surface in equation 10, however, may prove useful in discerning the influence of the number facesheet plies, impact energy, and impact velocity on the CAI residual strength. The regression results may be viewed schematically in the space of coded independent variables, as shown in figure 16.

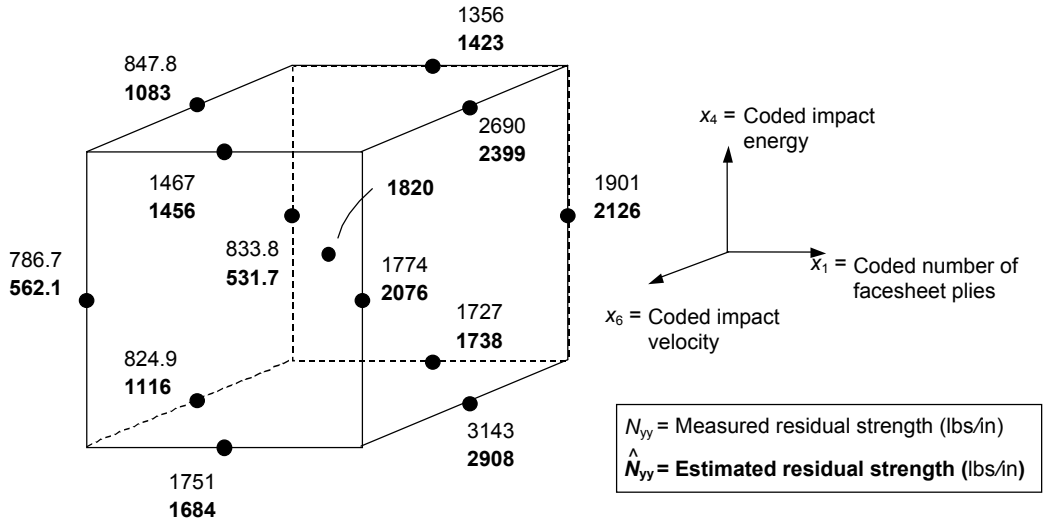

FIGURE 16. RESPONSE SURFACE ESTIMATES OF THE RESIDUAL STRENGTH AS A FUNCTION OF MATERIAL SYSTEM AND IMPACT PARAMETERS

Figures 17(a), 17(b), and 17(c) show the CAI residual strength predicted using equation 10 as a function of impact energy (X_4, x_4) and impact velocity (X_6, x_6) for the two-ply, four-ply, and six-ply facesheet configurations (or $x_1 = -1, 0, 1$), respectively. Similar to the results from the previous sections, a comparison of the three figures reveals that the predicted strength increases substantially as the number of facesheet plies is increased. In addition, the maximum CAI strength for a given combination of facesheet configuration and impact energy occurs at the midrange impact velocity; i.e., the CAI residual strength is somewhat rate dependent. The three contour plots are very nearly symmetric about a relative maximum or ridge in the predicted response occurring in the vicinity of the line, $X_6 = 96.30$ in/s ($x_6 = 0$). The magnitude of the estimated strength can decrease somewhat as the impact velocity is varied from the midrange test value ($x_6 = 0$) to either high or low values ($x_6 = \pm 1$). Lacy et al. [13] noted that the predicted planar damage dimension, D, was also a relative minimum along the line $x_6 = 0$ for the same set of test specimens. Hence, the residual strength is somewhat proportional to the size of the planar damage area. Sandwich panel stiffness properties, energy absorption capability, and support boundary conditions all play a key role in the dynamic impact response leading to damage development and loss of strength. This underscores the importance of adequately characterizing the expected impact scenarios when establishing a damage tolerance plan for sandwich composite aircraft structures.

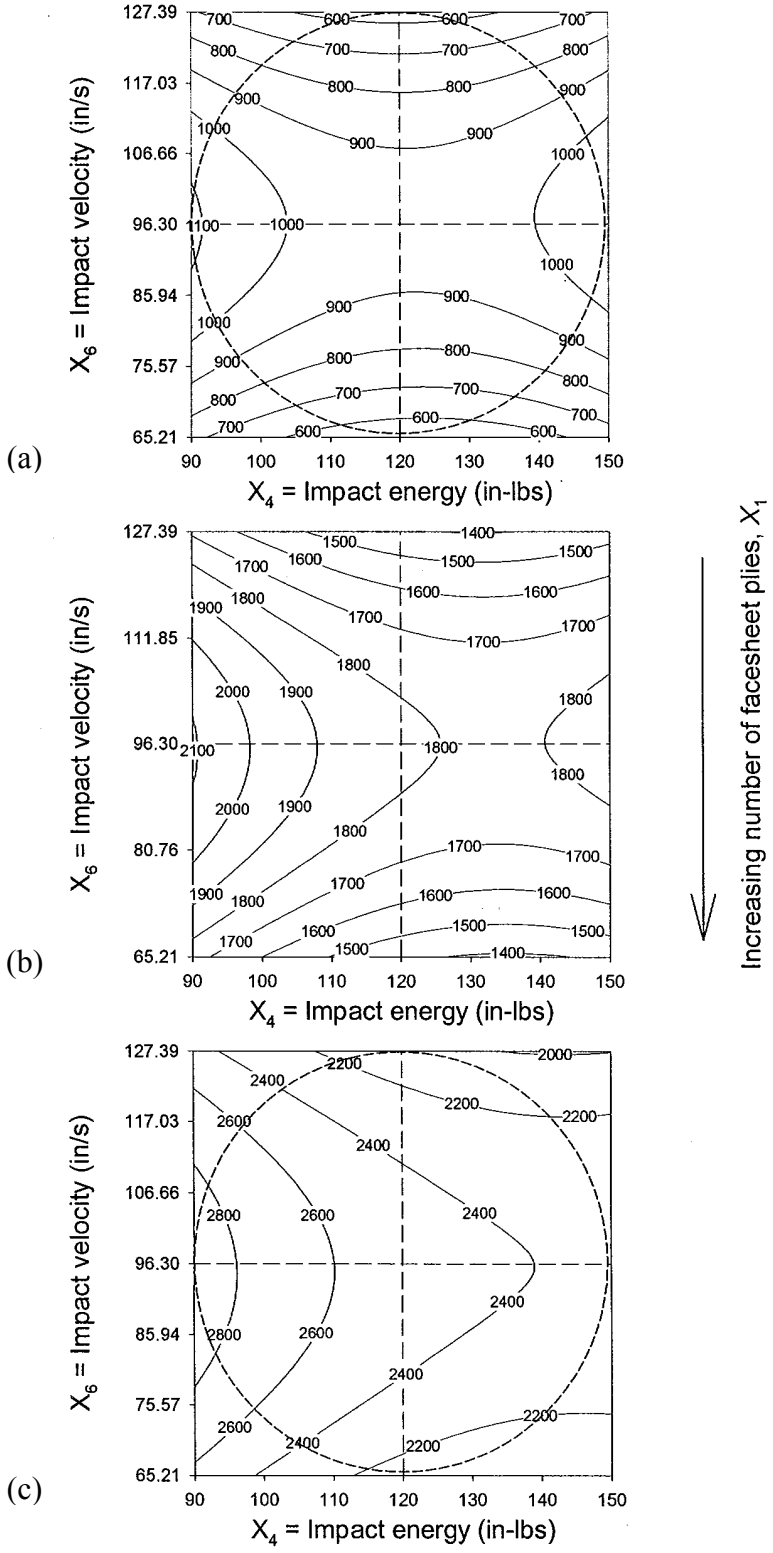

FIGURE 17. PREDICTED RESIDUAL STRENGTH (lbs/in): (a) X_1 = 2 plies $[90/45]_1$, (b) X_1 = 4 plies $[90/45]_2$, AND (c) X_1 = 6 plies $[90/45]_3$

The preceding results are in general agreement with the experimental observations. Figures 18 through 20 show the recorded CAI residual strengths for the test specimens corresponding to the midrange impact velocity ($x_6 = 0$; $X_6 = 2$ in), midrange impact energy ($x_4 = 0$; $X_4 = 120$ in-lbs), and midrange facesheet configurations ($x_1 = 0$; $X_1 = 4$ plies), respectively. Included with each observation is its associated TTU C-scan image and measured diameter, D, from reference 13. These figures show that the experimentally observed CAI strengths for a given facesheet configuration are consistent with the regressions of figure 16.

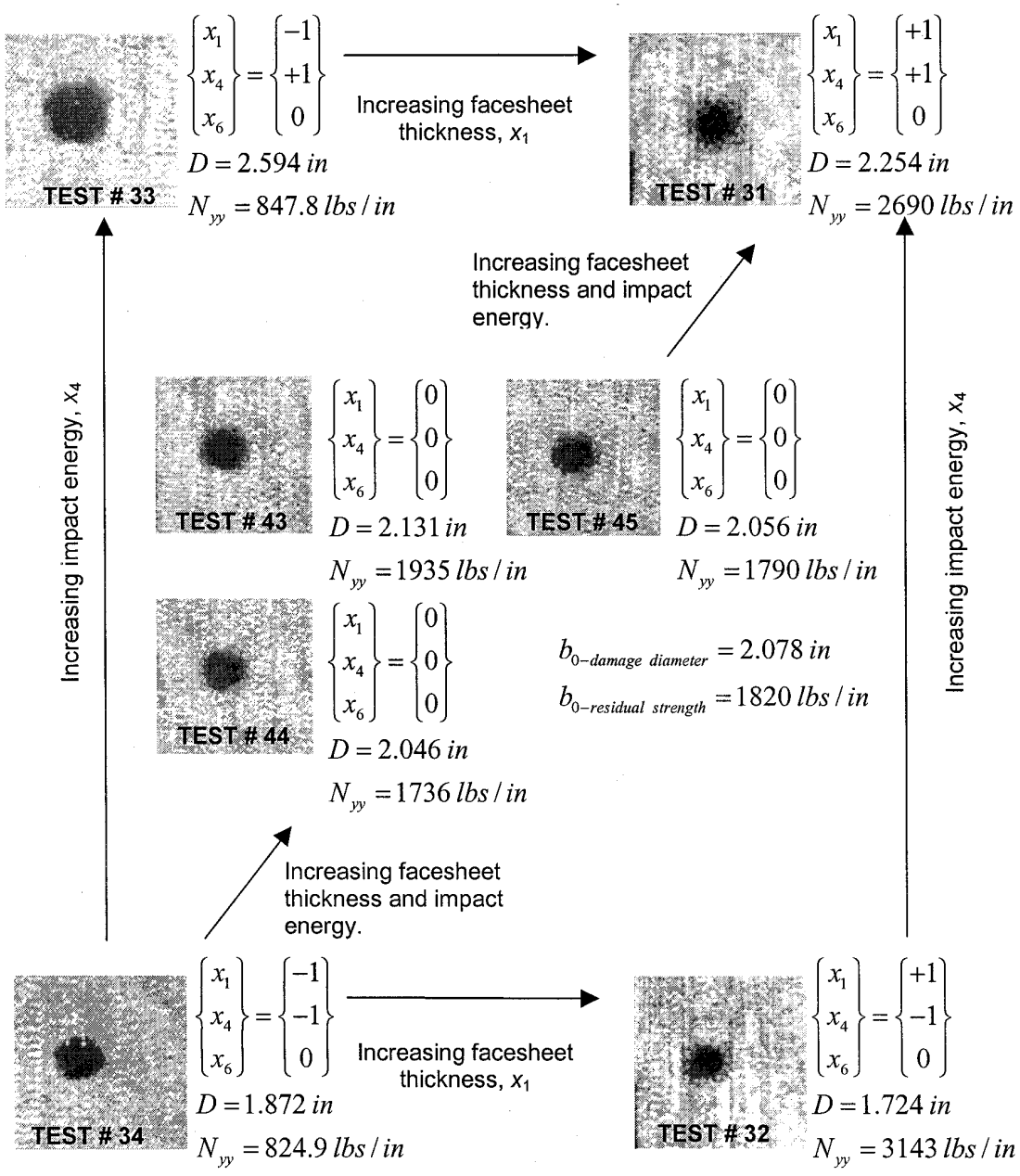

FIGURE 18. MEASURED DAMAGE DIAMETER [13] AND RESIDUAL STRENGTH FOR IMPACT VELOCITY, $X_6 = 96.30$ in/s ($x_6 = 0$)

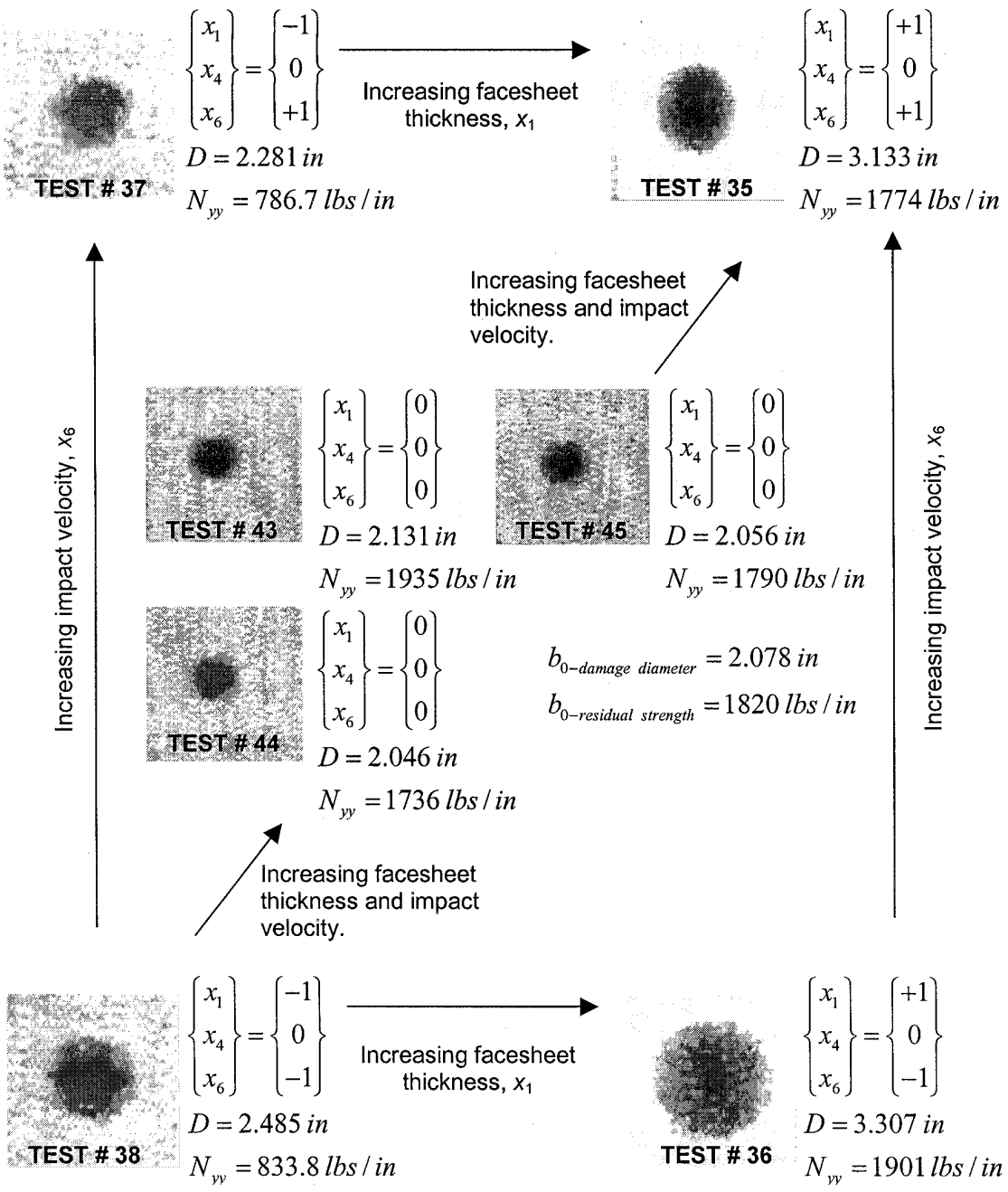

FIGURE 19. MEASURED DAMAGE DIAMETER [13] AND RESIDUAL STRENGTH FOR IMPACT ENERGY, X_4 = 120 in-lbs (x_4 = 0)

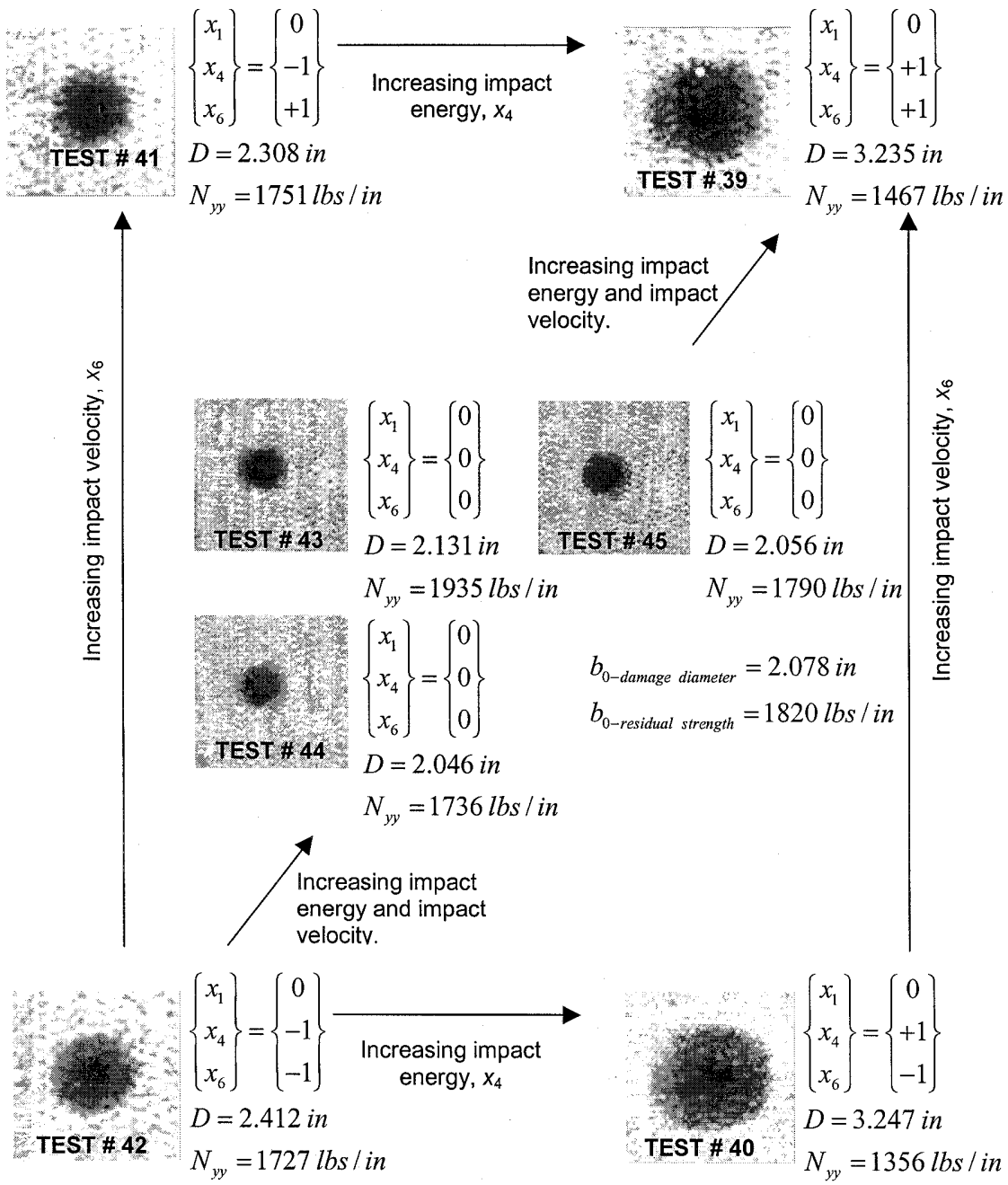

FIGURE 20. MEASURED DAMAGE DIAMETER [13] AND RESIDUAL STRENGTH FOR FACESHEET CONFIGURATION, X_1 = 4 plies $[90/45]_2$ ($x_1 = 0$)

For the test matrix, summarized in table 9, figure 21 contains a comparison of the response surface predictions of the TTU C-scan diameter from reference 13 to the response surface predictions of the normalized CAI residual strength developed in this examination. As noted earlier, the predicted normalized CAI residual strength for a given facesheet configuration is generally inversely proportional to the size of the planar damage area, D. This is consistent with the observations of Tomblin et al. [5] (cf., figure 3). A comparison of figures 21(d), 21(e), and

21(f) suggests that the CAI residual strength can range roughly between 50%-70% of the virgin panel strength for a given facesheet configuration.

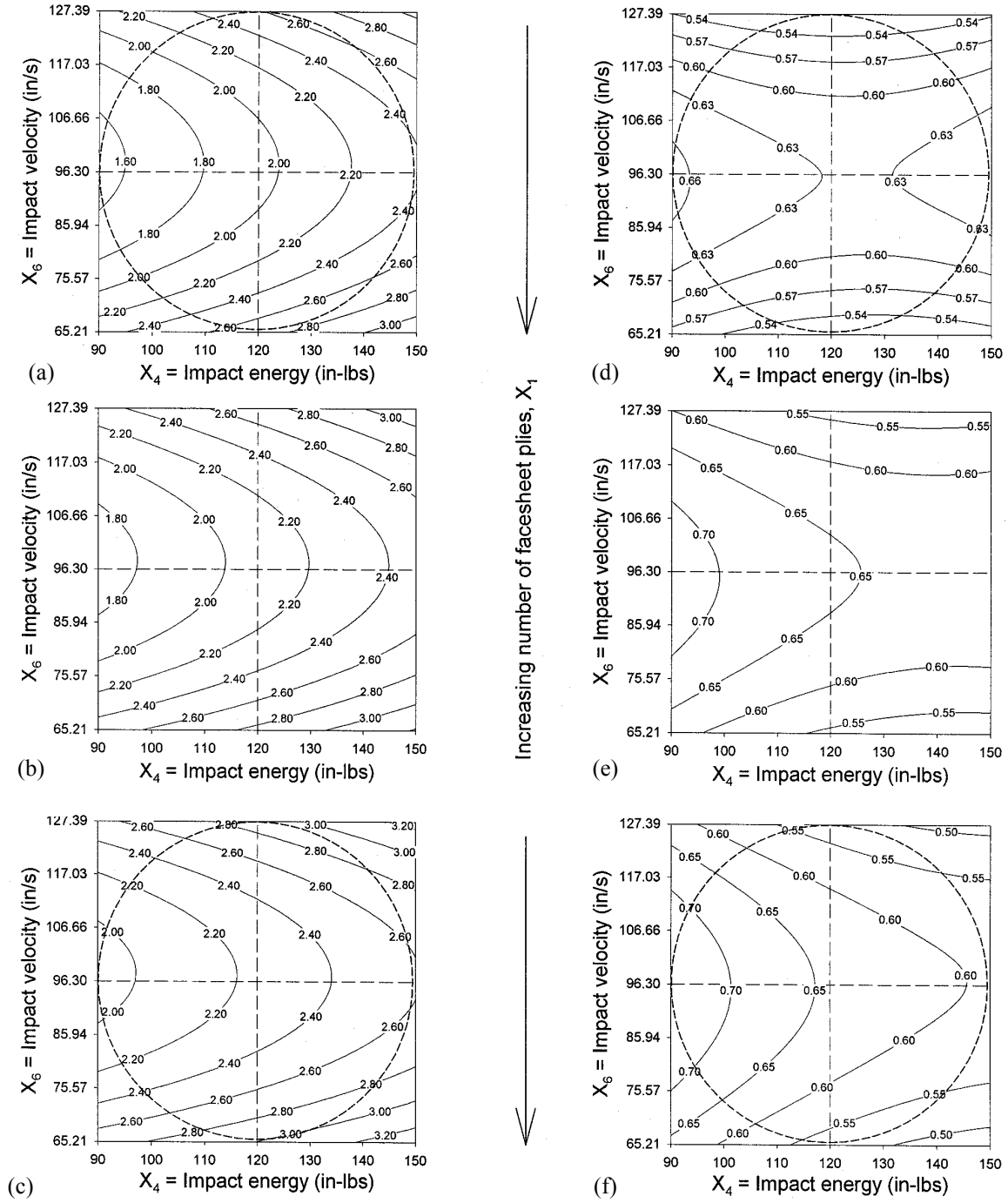

FIGURE 21. PREDICTED DAMAGE DIAMETER (in) FOR X_1: (a) TWO, (b) FOUR, AND (c) SIX PLIES [13]; PREDICTED NORMALIZED RESIDUAL STRENGTH FOR X_1: (d) TWO, (e) FOUR, AND (f) SIX PLIES

2.3.2 Correlation With Independent Experimental Results.

Table 10 contains a limited set of additional independent experimental results from Tomblin et al. [5], where the combination of configuration and impact variables lie within the spherical domain of the test matrix design used in this study. Response surface predictions of the planar diameter, $\hat{D}$, of the internal damage from reference 13 and the CAI residual strength (equation 10) are compared to measured damage diameters, D, from reference 13 in table 10. The measured and predicted CAI residual strengths are also compared in table 10. The difference between the experimentally measured strengths and the interpolated values varied between 1.4% and 23.4%, with a mean difference of 13.4%. Again, the difference between the experimentally measured CAI residual strengths and the estimated values using equation 10 was especially pronounced for x_1 = -1 (X_1 = 2 plies) where the residual strengths are greatly overpredicted.

TABLE 10. INTERPOLATION OF REGRESSION RESULTS IN THE SPACE OF CODED MATERIAL AND IMPACT VARIABLES

x_1	x_4	x_5	r	Measured Damage Diameter, D (in) [13]	Predicted Damage Diameter, $\hat{D}$ (in) [13]	$\left\|\frac{D-\hat{D}}{D}\right\|$ (%)	Measured Residual Strength, N_{yy} (lbs/in)	Predicted Residual Strength, $\hat{N}_{yy}$ (lbs/in)	$\left\|\frac{N_{yy}-\hat{N}_{yy}}{N_{yy}}\right\|$ (%)
0	0.30	-0.23	0.378	2.851	2.242	21.4	1708	1773	3.8
0	0.76	-0.08	0.764	2.531	2.381	5.9	N/A	N/A	N/A
0	-0.98	-0.14	0.990	2.022	1.750	13.5	1985	2095	5.5
-1	0.04	-0.02	1.001	1.996	1.965	1.5	822	945	14.9
-1	0.50	-0.11	1.123	2.784	2.178	21.8	785	968	23.4
1	0.63	-0.07	1.184	2.587	2.463	4.8	2365	2399	1.4
0	-1.18	-0.13	1.187	1.808	1.679	7.1	1827	2192	20.0
-1	-0.73	-0.11	1.243	2.283	1.663	27.2	846	1034	22.3
1	-0.86	-0.07	1.321	2.291	1.981	13.5	2453	2834	15.5

In the final part of this investigation, the coupled influence of the number of facesheet plies, impact energy, and impact velocity on the CAI residual strength was evaluated using empirically based response surfaces for sandwich composites comprised of carbon-epoxy woven fabric facesheets and Nomex honeycomb cores, where the core density, core thickness, and impactor diameter were held fixed in this examination. Lack of correlation between regression results and experimental observations for sandwich panels with two-ply facesheets suggests that quadratic response surfaces, such as equation 10, may have difficulty predicting the CAI strength for those test panels where facesheet penetration and/or bifurcation between failure modes are occurring. Similar to the results obtained using equations 7 and 9, response surface estimates of the CAI residual strength using equation 10 suggest that increasing the number of facesheet plies results in a significant improvement in the damage tolerance properties. Regression results suggest that damage development [13] and the CAI strength are somewhat sensitive to the velocity of the impactor. Midrange values of impact velocity resulted in strength estimates that were a relative maximum.

3. CONCLUSIONS AND RECOMMENDATIONS.

In this investigation, the influence of sandwich configuration and impact parameters on the damage tolerance characteristics of sandwich composites comprised of carbon-epoxy woven fabric facesheets and Nomex honeycomb cores was evaluated using empirically based response surfaces. A series of carefully selected tests were used to isolate the coupled influence of various combinations of the number of facesheet plies, core density, core thickness, impact energy, impactor diameter, and impact velocity on the compressive residual strength degradation in sandwich composites due to impact normal to the surface with relatively blunt spherical steel impactors. The ranges of selected material parameters were typical of those found in common aircraft applications. Quadratic response surface estimates of the CAI residual strength as a continuous function of material system and impact parameters were developed.

For a fixed set of impact parameters, response surface estimates of the CAI residual strength are highly sandwich configuration dependent. Regression results suggest that increasing the number of facesheet plies results in the greatest improvement in the damage tolerance properties. In addition, increasing the thickness of the core material can produce a significant increase in the predicted CAI strength. For sandwich panels where facesheet penetration was not a concern, residual strength estimates generally were inversely proportional to the size of the planar damage region obtained from a previous study. The developed response surface for the residual strength for the above set of impact parameters was sufficiently accurate considering the scatter of the test data used to develop the response surface.

In addition, the experimental results and regression analysis suggest that impact damage development and loss of strength in sandwich composites is highly sensitive to the diameter of the impactor, impact energy, and impact velocity. An increase in the impact energy and/or impactor diameter generally resulted in a decrease in the CAI residual strength for those cases where facesheet penetration was not likely. Moreover, response surface results indicate that the damage formation and loss of strength is somewhat sensitive to the velocity of the impactor. Sandwich panel stiffness properties, energy absorption capability, and support boundary conditions all play a key role in the dynamic impact response leading to damage development.

For a given range of sandwich configuration and impact parameters, response surfaces may be used to estimate the size of the ensuing impact damage as well as the degradation in residual strength. Special care should be taken when estimating the CAI residual strength for cases where the range of independent variables spans a potential bifurcation between failure modes. This occurs primarily for thin facesheets and sharp impactors. A response surface for two diameters and two facesheet thicknesses may be too narrow in scope to be of any practical use. In general, the response surfaces for the compressive residual strength developed here can be of qualitative use, but are not as useful as those developed for damage resistance.

To fully develop the concepts outlined here, a detailed risk assessment establishing impact scenarios that represent a viable threat to principle structural elements is required prior to establishing a damage tolerance plan. Such an assessment would likely involve specifying the upper bounds on the impact parameters (impact energy, impact velocity, and impactor diameter) that represent a realistic threat to a given structural component. It is important that the structural

integrity is not seriously degraded by any impact damage falling below the threshold of detectability using standard detection techniques.

4. REFERENCES.

1. Allen, H.G., "Analysis and Design of Structured Sandwich Panels," Pergammon Press, Oxford, 1969.

2. Plantema, F.J., "Sandwich Construction," Wiley, Chinchester, 1966.

3. Vinson, J.R., "The Behavior of Sandwich Structures of Isotropic and Composite Materials," Technomic, Lancaster, 1999.

4. Tomblin, J., Lacy T., Smith, B., Hooper, S., Vizzini, A., and Lee, S., "Review of Damage Tolerance for Composite Sandwich Airframe Structures," DOT/FAA/AR-99/49, August 1999.

5. Tomblin, J.S., Raju, K.S., Liew, J. and Smith, B.L., "Impact Damage Characterization and Damage Tolerance of Composite Sandwich Airframe Structures," DOT/FAA/AR-00/44, January 2001.

6. Abrate, S., "Impact on Laminated Composite Materials," *Appl. Mech. Rev.*, 44(4), pp. 155-190, 1991.

7. Abrate, S., "Impact on Laminated Composites: Recent Advances," *Appl. Mech. Rev.*, 47(11), pp. 517-544, 1994.

8. Abrate, S., "Localized Impact on Sandwich Structures with Laminated Facings," *Appl. Mech. Rev.*, 50(2), pp. 69-82, 1997.

9. Russell, S.G., Lin, W., Kan, H.-P., and Deo, R.B., "Damage Tolerance and Fail Safety of Composite Sandwich Panels," S*AE Transactions, Journal of Aerospace*, 103, pp. 2175-2182, 1994.

10. Noor, A.K., Burton, W.S., and Bert, C.W., "Computational Models for Sandwich Panels and Shells," *Appl. Mech. Rev.*, 49(3), pp. 155-199, 1996.

11. Sierakowski, R.L. and Newaz, G.M., "Damage Tolerance in Advanced Composites," Technomic, Lancaster, 1995.

12. Tomblin, J.S., Raju, K.S., Acosta, J.F., Smith, B.L., and Romine, N.A., "Impact Damage Characterization and Damage Tolerance of Composite Sandwich Airframe Structures Phase II," DOT/FAA/AR-02/80, September 2002.

13. Lacy, T.E., Samarah, I.K., and Tomblin, J.S., "Damage Resistance Characterization of Sandwich Composites Using Response Surfaces," DOT/FAA/AR-01/71, March 2001.

14. Box, G.E.P. and Behnken, D.W., "Some New Three Level Designs for the Study of Quantitative Variables," *Technometrics*, 2(4), pp. 455-475, 1960.

15. Box G.E.P., Hunter W.G., and Hunter J.S., "Statistics For Experiments," Wiley & Sons, New York, 1978.

16. Montgomery D.C., "Design and Analysis of Experiments," Wiley & Sons, New York, 1991.

17. Myers R. and Montgomery D.C., "Response Surface Methodology," Wiley & Sons, New York, 1995.

18. Neter J., Wasserman W., and Kunter H.M., "Applied Linear Statistical Models, 3rd Edition," Irwin, Homewood, IL, 1990.

19. Khuri A.K. and Cornel J.A., "Response Surfaces," Marcel Dekker, Inc., 1987.

20. Saczalski, T.K., "Determination of Multivariable G_{Ic} and G_{IIc} Fracture Toughness Response Functions for Fiber/Resin Composite," *Proceed*ings *of the 34th International* S*AMPE* S*ymposium and Exhibition*, pp. 726-736, 1989.

21. Saczalski, T., Lucht, B., and Steeb, D., "Advanced Experimental Design Applied to Damage Tolerance of Composite Materials," *Proceed*ings *of the 23rd International* S*AMPE Conference*, Kiamesha Lake, NY, Oct. 21-24, 1991.

22. Saczalski, T., Lucht, B., and Saczalski, K., "Experimental Design Methods for Assessment of Composite Damage in Recreational Structures," *Composite Materials: Fatigue and Fracture*, Vol. 6, pp. 45-69, 1997.